

Published in final edited form as:

*Protein Pept Lett.* ; 3(10): 567–588. doi:10.1038/s41570-019-0129-8.

## Hierarchically oriented organization in supramolecular peptide crystals

Chengqian Yuan<sup>#1</sup>, Wei Ji<sup>#2</sup>, Ruirui Xing<sup>1</sup>, Junbai Li<sup>\*,3,4</sup>, Ehud Gazit<sup>\*,2,5</sup>, Xuehai Yan<sup>\*,1,4,6</sup>

<sup>1</sup>State Key Laboratory of Biochemical Engineering, Institute of Process Engineering, Chinese Academy of Sciences, Beijing, China

<sup>2</sup>Department of Molecular Microbiology and Biotechnology, George S. Wise Faculty of Life Sciences, Tel Aviv University, Tel Aviv, Israel

<sup>3</sup>Beijing National Laboratory for Molecular Sciences (BNLMS), CAS Key Lab of Colloid, Interface and Chemical Thermodynamics, Institute of Chemistry, Chinese Academy of Sciences, Beijing, China

<sup>4</sup>University of Chinese Academy of Sciences, Beijing, China

<sup>5</sup>Department of Materials Science and Engineering, Iby and Aladar Fleischman Faculty of Engineering Tel Aviv University, Tel Aviv, Israel

<sup>6</sup>Center for Mesoscience, Institute of Process Engineering, Chinese Academy of Sciences Beijing, China

# These authors contributed equally to this work.

### Abstract

Hierarchical self-assembly and crystallization with long-range ordered spatial arrangement is ubiquitous in nature and plays an essential role in the regulation of structures and biological functions. Inspired by the multiscale hierarchical structures in biology, tremendous efforts have been devoted to the understanding of hierarchical self-assembly and crystallization of biomolecules such as peptides and amino acids. Understanding the fundamental mechanisms underlying the construction and organization of multiscale architectures is crucial for the design and fabrication of complex functional systems with long-range alignment of molecules.

This Review summarizes the typical examples for hierarchically oriented organization of peptide self-assembly and discusses the thermodynamic and kinetic mechanisms that are responsible for this specific hierarchical organization. Most importantly, we propose the concept of hierarchically

---

\* jbli@iccas.ac.cn; ehudg@post.tau.ac.il; yanxh@ipe.ac.cn.

#### Author contributions

C.Y. and W. J. contributed equally to this work. X.Y., J.L. and E.G. conceived the Review. All authors contributed to the discussion and writing of the Review.

#### Competing interests

The authors declare no competing interests.

#### Peer review information

*Nature Reviews Chemistry* thanks T. Tuttle, R. Ulijn and B. Nilsson for their contribution to the peer review of this work.

#### Publisher's note

Springer Nature remains neutral with regard to jurisdictional claims in published maps and institutional affiliations.

oriented organization for self-assembling peptide crystals, distinct from the traditional growth mechanism of supramolecular polymerization and crystallization based on the Ostwald ripening rule. Finally, we assess critical challenges and highlight future directions towards the mechanistic understanding and versatile application of the hierarchically oriented organization mechanism.

---

Complex superstructures made by hierarchical self-assembly or crystallization are ubiquitous in biological systems, with prominent examples including actin filaments, annulus fibrosus, microtubules and filamentous viruses. The ordered organization of these structures plays essential roles in facilitating functionality<sup>1-3</sup>. For example, the bundling or oriented organization of nanostructures self-assembled from molecular building blocks regulates biological processes such as protein transport, signal transduction and cell division. As a key structural protein in eukaryotic cells, actin has been selected as a typical building block for investigations of biopolymer hierarchical self-assembly<sup>4-6</sup>. It has been found that bundles or paracrystals can be condensed from actin rods in the presence of sufficiently high concentrations of multivalent ions<sup>6</sup>. In addition, the development of materials that are simultaneously tough and flexible is usually associated with their hierarchically oriented arrangement, such as laminated organization and hexagonal packing<sup>7</sup>. Moreover, supramolecular architectures with higher-order organization can also be used to direct charge carriers in inorganic semiconductors in transistors or photovoltaic devices. However, designing and generating complex functional systems with long-range alignment of molecules in a spatiotemporally controlled manner remains a great challenge. Therefore, a fundamental understanding of the mechanisms to achieve hierarchical self-assembly and crystallization is crucial to advance their important applications.

Peptides and their derivatives, consisting of dozens of amino acids, have attracted widespread attention as biological and bio-inspired building blocks owing to their outstanding applications in the construction of advanced functional materials for nanotechnology and biomedicine<sup>8</sup>. Owing to their outstanding advantages — such as inherent biological origin, low immuno-genicity, biocompatibility and versatile functionality — self-assembled peptide supramolecular nanostructures provide promising platforms for the understanding and rational design of multifunctional materials featuring hierarchical superstructures<sup>9,10</sup>. In the past decades, many efforts have been devoted to the preparation of such sophisticated structures exhibiting long-range order using diverse methodologies, such as X-ray irradiation<sup>11</sup>, phase transformation<sup>12</sup>, solvent thermal annealing<sup>13</sup>, spinning of aligned supramolecular nanotubes<sup>14</sup> and external field-induced alignment<sup>15</sup>. These well-defined nanostructures could further assemble into higher-ordered assemblies, including even nanoscale crystals. However, no comprehensive report that summarizes the progress on the oriented, multiscale hierarchical self-assembly of peptides and provides theoretical insights into the underlying mechanism has been presented to date.

Herein, we intend to introduce the concept of hierarchically oriented organization as a general principle for the hierarchical self-assembly and crystallization of peptides and other organic molecules. First, we present the typical examples of hierarchical peptide structures self-assembled through oriented organization, and their diverse properties. Then, we analyse the fundamental thermodynamics and kinetics underlying the self-assembly crystallization

mechanisms of peptides (FIG. 1). Finally, we discuss the future trends and challenges of hierarchical self-assembly and oriented crystallization from various molecular building blocks, including peptides and amino acids, for the fabrication of bio-inspired materials using multiscale structures.

## Peptide self-assembly and crystallization

### Linear short peptides

The precise design and construction of biomimetic systems requires a deeper understanding of the self-assembly pathways and of the mechanisms underlying the formation process. However, bio-inspired materials based on natural systems composed of complex building blocks, such as proteins, are difficult to implement. Therefore, building blocks based on simple and short linear peptides have been designed and selected to self-assemble into different nanostructures. Some of the most prominent examples include lanreotide<sup>16</sup>, a synthesized octapeptide used as a growth hormone inhibitor, and diphenylalanine (FF)<sup>17</sup>, a core sequence that mediates the fibrillation of Alzheimer disease's amyloid- $\beta$  (A $\beta$ ). Extensive studies have shown that various nanostructures, including nanotubes<sup>17</sup>, nanofibres<sup>18</sup>, nanowires<sup>19</sup> and vesicles<sup>20</sup>, can be generated from FF-based building blocks. However, the organization of these nanostructures into macroscopic-ordered structures, such as crystalline materials with certain spatial configurations, still remains a formidable challenge. We have previously attempted the preparation of hexagonal FF microtubes through solvent thermal annealing<sup>13</sup>. The diameters of the designed microtubes were in the order of micrometres, with a length of several millimetres. Moreover, we could control the assembly and disassembly of the microtubes into nanotubes by increasing and decreasing the concentration of FF, respectively (FIG. 2a). This work provides an alternative approach to fabricate hexagonal peptide microtubes through hierarchically oriented organization of the basic molecular building block. FF microtubes with similar hierarchical organization have also been prepared through a capillary-driven assembly process and observed by high-magnification scanning electron microscopy and polarized optical microscopy<sup>21</sup>. In addition to 1D microstructures and nanostructures, 3D peony-flower-like hierarchical mesocrystals have also been produced in tetrahydrofuran from the assembly of primary flakes<sup>22</sup>. Atomic force microscopy (AFM) analyses of the flakes' surface defects clearly revealed that each flake consisted of multilayer structures. It should be noted that the surface of the single layer, with an average lamellar thickness of 1.1–1.2 nm, was quite smooth. Moreover, thicker flakes could be further generated with the assistance of hydrogen bond donor solvents, as confirmed by the lamellar thickness measured by X-ray powder diffraction and AFM. Such a hierarchically oriented organization methodology can be used as an effective approach to obtain 3D superstructures from simple peptide building blocks, aiming to fully realize their potential applications in biotechnological fields.

With the development of molecular self-assembly and nanotechnology, the research focus has changed from the crystalline structures to their corresponding functions. However, the design of superstructures that are simultaneously flexible, strong and tough remains a big challenge. In some biological systems, such as bones and nacre, hierarchically oriented architectures and the resulting anisotropy endow the superstructures with remarkable

mechanical properties. Inspired by nature, we have explored the mechanical properties of hierarchical self-assembled architectures of short peptides such as *tert*-butoxycarbonyl (Boc)-FF<sup>7</sup>. This is a popular building block in nanotechnology and self-assembled Boc-FF structures exhibit various properties similar to graphene and seem to be promising for applications in biomedical engineering and as bioinspired composites. After evaluation of the mechanical properties of the individual crystal assisted by density functional theory calculations, Boc-FF crystals were found to exhibit well-ordered molecular organization stabilized by a network of hydrogen bonding and aromatic interactions alongside unique elastic flexibility. Scanning electron microscopy analyses showed that the crystals were composed of stacked layers bound by weak interactions, which may be responsible for the material being simultaneously strong, tough and flexible (FIG. 2b). These Boc-FF crystals represent the simplest form of anisotropic self-assembled materials, bearing great potential in applications requiring contradictory mechanical properties. In fact, lamination has been used as an effective approach to obtain alloys that are both tough and flexible, such as Damascus steel and Japanese Katana<sup>23</sup>.

Self-assembling crystalline nanostructures composed of other short peptides, such as PFF, DYF, YFD, 9-fluor-enylmethoxycarbonyl (Fmoc)-GG, acetylated IVE, acetylated LLE-NH<sub>2</sub>, acetylated LVE, KLVFF and A<sub>6</sub>K, have also been shown to emerge as a result of hierarchically oriented substructures<sup>24–31</sup>. For instance, the acetylation of KLVFF, namely fragment A $\beta$ (16–20), can lead to rapid self-assembly into macroscopic lamellar structures composed of an oriented stacking of the microcrystals. The single lamellae are 2D with nanoscale thickness, and their further stacking results in the compact microcrystal<sup>27</sup> (FIG. 2c). Interestingly, large fibre bundles were formed from the lateral association of primary fibres and the same laminated organization was also observed in the Fmoc-GG and Fmoc-FF self-assembled systems<sup>28</sup>. It can be concluded that the lamellar structure is commonly obtained in short-peptide-based self-assembling systems. In addition to the simplest hierarchical organization form, hexagonal liquid crystal phases were recently reported to spontaneously form through oriented organization of rigid helical nanofilaments self-assembled by highly charged peptides<sup>32</sup>. Intriguingly, such an oriented organization was also found in the crystal growth of smaller biomolecules, namely amino acids and their derivatives<sup>33–37</sup>. For example, a compact single crystal was formed through the fusion of DL-alanine mesocrystal nanoparticles (FIG. 2d). This was evidenced by the structural changes before and after formation of a single crystal observed using time-dependent dynamic light scattering and smallangle neutron scattering<sup>33</sup>. Another study conducted in a water–isopropyl alcohol mixture revealed that the alanine microcrystal, comprising pores and a rough surface, was assembled from aligned layers<sup>34</sup>. Therefore, the multistep hierarchically oriented organization of peptides may be a crystallization growth mechanism alternative to the classical one.

In addition to self-assembly in solution, a diversity of architectural motifs with unique properties was obtained through constrained assembly on solid surfaces<sup>38–40</sup>, yet the molecular mechanisms of their nucleation and growth remain elusive. The nucleation of 2D arrays was investigated through direct observation by in situ AFM and molecular dynamics simulations of a heptapeptide (YSATFTY) exhibiting strong binding affinity to molybdenum disulfide<sup>41</sup>. It was found that the nucleation was a free energy barrier process and the

arrays assembled one row at a time (FIG. 2e). This study provides direct evidence for the long-standing, yet so far unproven, predictions of the classical nucleation theory for the emergence of order and post-nucleation growth<sup>42</sup>, and demonstrates the key interactions underlying 2D assembly.

Formation of self-assembled fibrillary hydrogels and formation of ordered crystals are related processes, both involving similar events such as molecular-level association, dissociation and rearrangement. However, the relationship between fibril growth and crystal growth remains elusive. To elucidate this issue, a study was performed to investigate the structural transformation from hydrogel to crystals of Fmoc-*p*-nitrophenylalanine (Fmoc-4-NO<sub>2</sub>-F), a phenylalanine derivative. Time-dependent transmission electron microscopy (TEM) images show that fibrils 11.9±2.0 nm in diameter and several micrometres in length were formed upon the initiation of hydrogel formation. Within a short period of time (10–30 min), thicker fibril bundles were generated due to lengthwise alignment and fusion. With the increasing degree of fibril fusion, the width of the fibril bundles reached several hundred nanometres and the resulting assemblies appeared to display a rigid geometry with evident curvature. Subsequently, nanocrystalline aggregates and hollow crystalline microtubes were formed after 30 minutes and 12 hours, respectively. This process clearly demonstrates that the crystal evolved from the alignment and fusion of hydrogel fibrils, rather than from the dissociation of monomers from the fibrils. Thus, the molecular orientation within the resulting crystals and the hydrogel fibrils can be expected to retain the same linear arrangement. This further confirms that crystals are formed through the hierarchically oriented rearrangement of the nanofibres. Moreover, this finding also reveals that the hydrogel fibrils formed at the early stage are kinetically trapped, whereas the formation of crystalline microtubes is thermodynamically favourable<sup>43</sup>. Further experimental observations reveal that such a rule governing peptide crystallization is also applicable to other Fmoc-phenylalanine derivatives and corresponding peptide analogues, such as those substituted by fluoro and nitro groups<sup>44–46</sup>.

### External field-induced oriented alignment

Amino acid and peptide-based hydrogels are promising scaffolds for artificial organs and tissues; however, their structures consist of supramolecular polymer networks of random orientation, far removed from the anisotropic hierarchical multiscale structure of their natural counterparts. Notably, the anisotropic structure at the macroscale is critical for specific biological functions, such as birefringence, bireflection and polarization emission, that depend on anisotropic mechanical and optical properties. Therefore, external field-assisted approaches aimed at generating biomimetic hierarchical self-assemblies have become appealing. Recently, ultrasonic irradiation has been used to induce a hierarchical orientation of flexible nanofibres, which were transformed from the triclinic aggregates of a bioinspired dipeptide, and produce crystalline nanobelts exhibiting strong polarized luminescence<sup>47</sup>. During this transition process, the weak interactions involved in kinetically trapped phase states, such as hydrophobic and self-locked intramolecular hydrogen bonds, can be cleaved with the assistance of cavitation effects, and the subsequent molecular rearrangement generates another well-ordered crystalline structure with a higher thermodynamic stability.

Ultrasonication-assisted self-assembly can serve as an effective *in situ* strategy to obtain anisotropic nanostructures such as aligned hydrogels. Ulijn and colleagues demonstrated the generation of anisotropic organogels and hydrogels with aligned tripeptide (<sup>D</sup>FFD and <sup>D</sup>FFI) nanostructures based on sonication-induced assembly<sup>48</sup> (FIG. 3a). TEM images showed the structural evolution from disordered short nanofibres to highly oriented fibrous clusters following ultrasound treatment. Such a strategy based on sonication-modulated hierarchical self-assembly may give rise to rearrangement of the molecular organization associated with distinct molecular interactions.

Other external fields, such as electric fields, were also employed to tune the orientation and alignment of the initial nanostructures to achieve highly ordered macro-structures. External electric fields have been used to induce the formation of electric dipoles along silk nanofibres that then attract or repel each other. Electrostatic attraction dictates the alignment of nanofibres along one direction, whereas electrostatic repulsion dictates the separation of the aligned nanofibres into layers, hence leading to the formation of hierarchical anisotropic structures<sup>49</sup> (FIG. 3b). Similarly, an external magnetic field could also induce the formation of aligned aromatic peptide nanotubes regardless of the presence of a ferrofluid. This arrangement can be attributed to the diamagnetic anisotropy resulting from the well-ordered stacking and orientation of the aromatic rings<sup>15,50</sup> (FIG. 3c).

The application of shear force can also trigger the long-range ordered macroscopic alignment of peptides<sup>51–53</sup>. For instance, noodle-like peptide hydrogel strings were formed under the shear force produced at the point of injecting the peptide solution into a phosphate-buffered saline solution<sup>51</sup> (FIG. 3d). Bulk birefringence revealed the anisotropy of the hydrogel alignment. Similarly, other hydrogels with oriented arrangement induced by external force have been produced, such as supramolecular silk and aligned macroscopic domains from peptide hydrogels<sup>52,53</sup>. It should be noted that the external forces determine the direction of the alignment and orientation of the nanotubes, hence generating the anisotropic hydrogel on a macroscopic scale. Therefore, external forces enable the formation of multiscale hierarchical materials with well-ordered anisotropic structures and effectively span the utility of peptide hydrogels, such as in the case of bioinspired silk fibrils.

*In vivo*, once the initial protein fibres further organize into higher-order assemblies, such as plaques and tangles, various degenerative diseases may develop. Therefore, research on the different factors, such as internal or environmental conditions, affecting the kinetics of the self-assembly process associated with the formation of degenerative diseases has gained considerable interest. In this context, a study focusing on the construction of nanofibres from an A $\beta$  peptide derivative and the modulation of their higher-order assembly into different microstructures and nanostructures through tuning the internal or environmental factors was conducted. The A $\beta$ -derived peptide, Nap-RGDFF-OH, was selected as a building block to self-assemble into A $\beta$  fibres<sup>54</sup>. Distinct microstructures and nanostructures, such as plaques and tangles that mimic the pathological A $\beta$  deposits, were attained by modulating the hierarchical self-assembly of the peptide nanofibres via tuning the concentration, temperature, time and pH. The model peptide was found to exhibit obvious concentration-dependent hierarchical self-assembly behaviours. Specifically, the A $\beta$  nanofibre could evolve into microsheets and nanosheets in a hierarchically oriented manner when the



peptide concentration was increased from 1 mg ml<sup>-1</sup> to 15 mg ml<sup>-1</sup> (REF.<sup>54</sup>). Moreover, Li and co-workers found that the ultralong aligned FF single crystals display a smooth surface and a pronounced terrace topology, indicating that this peptide also crystallizes in a hierarchically organized manner<sup>55</sup>. Hierarchical self-assembly synergistically controlled by kinetics and thermodynamics was also realized by modulating the peptide sequence or the self-assembly kinetic parameters<sup>56</sup>. For example, hierarchical hexagonal microtubules could be modulated by changing the ratio between the FF concentration and the relative humidity (RH) in the growth chamber (defined as the FF:RH ratio)<sup>57</sup>. Hexagonal nanotubes with opposite charges at both ends were initially formed through hexagonal arrangement of the FF molecules when an electric field was applied to the nanotubes. Subsequently, hierarchically structured hexagonal microtubules were generated under the synergy of side-by-side hexagonal aggregation and end-to-end elongation. Moreover, it was found that assemblies exhibiting different extents of crystallinity ranging from amorphous structures to more ordered ones formed at different FF:RH ratios give rise to different initial numbers of nanotubes, hence leading to microtubules with different morphologies. This strategy will advance our understanding of peptide self-assembly polymorphism and facilitate the rational design and development of functional materials for biomedical applications.

### Cyclic peptides

Cyclic peptides have attracted much attention in diverse fields ranging from self-assembling nanomaterials to drugs and chemical biology tools owing to their extraordinary high mechanical strength, toughness and elasticity<sup>58–60</sup>. Cyclic peptides are often found in bioactive natural products and can effectively mimic the peptide motifs involved in specific protein–protein interactions. Moreover, the remarkable structural rigidity and superior tendency to form hydrogen bonds endow the cyclic peptides with improved metabolic stability and bioavailability compared with their linear counterparts. As the smallest naturally occurring cyclic peptides, cyclic dipeptides (CDPs) have attracted tremendous attention owing to their exceptional biological and pharmacological activities as, for example, antitumour antimicrobial drugs and as immune regulators. Over the past decades, CDPs have been demonstrated to form molecular chain or layer stacks through the formation of N–H•••O hydrogen bonds between neighbouring molecules<sup>61,62</sup>. Considering the structural rigidity, responsivity, biocompatibility and degradability of cyclic peptides, it would be fascinating to construct biocompatible hierarchical higher-ordered structures with complex functions. To this end, we have previously reported the hierarchically oriented crystallization of self-assembled fibrous FF networks triggered by aldehyde<sup>63</sup>. The role of aldehyde during such a process can be addressed in two aspects. First, the intramolecular cyclization of linear FF dipeptides is triggered by the Schiff's base formed between the FF and aldehyde molecules, facilitating the formation of cyclic FF. Second, the presence of aldehyde induces the formation of crosslinked spherical structures, thus destroying the gel networks and accelerating the phase transition from gel to crystal. The crystalline structures were stabilized by cooperative intermolecular interactions of  $\pi$ – $\pi$  stacking and hydrogen bonds. The resulting platelets showing 3D-ordered organization were oriented along the longitudinal axis. Such peptide crystals displaying hierarchically oriented organization exhibited outstanding thermal stability and optical waveguiding properties (FIG. 4a). It should be noted that the assembly process is determined by intramolecular cyclization

and kinetically controlled crystallization, in which the later process usually requires at least 1 month<sup>63</sup>. An alternative strategy based on solvothermal treatment was developed to accomplish the cyclization and subsequent crystallization within 10 min (REF.<sup>64</sup>) This is ascribed to the enhanced phase separation of gels and accelerated cyclization kinetics accompanied by subsequent nucleation, growth and crystallization. Furthermore, a small amount of formaldehyde was shown to effectively increase the thickness of the crystalline nanobelts. More interestingly, such crystalline platelets of length in the order of hundreds of micrometres were capable of curved optical waveguiding, which has potential applications in bio-optics and optoelectronics<sup>64</sup>.

In addition to the intrinsic luminescence caused by the quantum confinement effect<sup>65</sup>, other functional moieties, such as azobenzene and naphthalenediimide, have been coupled to cyclic peptides to explore new supramolecular architectures and functionalities<sup>66,67</sup>. For example, 10,12-pentacosadiynoic acid, a photopolymerizable monomer, was covalently attached to a series of CDPs, including cyclo-(GS) and *cis/trans* cyclo-(SS). Morphology and X-ray diffraction analysis revealed that self-assembly of such CDP–10,12-pentacosadiynoic acid conjugates yielded single-wall and multiwalled nanotubes that evolved from the well-ordered lamellar structures, with an interlamellar distance of 6–7 nm. Moreover, upon UV irradiation, self-assembling CDP–10, 12-pentacosadiynoic acid tubes transformed into bluecoloured CDP–polydiacetylene nanotubes without any structural damage. Intriguingly, a reversible colour change of the CDP–polydiacetylene nanotubes between blue and red was observed for more than 10 consecutive thermal cycles. The CDP–10,12-pentacosadiynoic acid and CDP–polydiacetylene supramolecular system provides insights into the design and development of stimulus-responsive functional materials with a diverse range of applications<sup>68</sup>.

Despite the advances of CDP self-assembly, controlled fabrication of CDP nanostructures, especially the formation of higher-order self-assemblies, is still challenging, possibly due to the absence of suitable  $\alpha$ -substituents. Previous studies on symmetrically substituted diketopiperazines have demonstrated that the presence of  $\alpha$ -substituents increases the intermolecular interactions (such as hydrogen bonds and  $\pi$ – $\pi$  stacking) that facilitate the generation of higher-order extended structures<sup>69</sup>. The absence of  $\alpha$ -substituents can be compensated by orthogonal non-covalent interactions, such as  $\pi$ – $\pi$  stacking. Prominent examples include the design and assembly of such CDP molecules, which self-assembled into layered nanostructures and microstructures<sup>70–72</sup> (FIG. 4b,c).

Cyclic peptide nanotubes with different diameters and structures can be obtained through rational design of the chemical structures. Molecular clusters of cyclic peptides with flat and ring-shaped conformations are mainly connected through hydrogen bonds between amide groups. In general, cyclic peptide self-assembly in aqueous media is initiated by an abrupt solubility change of the peptide, followed by an oriented crystallization of the nanotubes<sup>58</sup>. However, understanding of the effect of the medium on the cyclic peptide self-assembly remains elusive. To this end, a pioneering study was conducted to investigate the self-assembly behaviour of cyclic peptides in a nematic liquid crystal medium<sup>73</sup>. Hexagonal hollow tubes were obtained, with diameters in the order of micrometres and lengths of several millimetres. Experimental evidence revealed that the microtubes formed



through a hierarchical oriented organization manner. Hexagonal nanotubes were first formed through the stacking of individual lipophilic macrolactam cyclo-(NHCH<sub>2</sub>CH=CHCH<sub>2</sub>CO)<sub>3</sub> (E-olefin) molecules, which then self-organized into higher-order assemblies. Hydrogen bonds were critical for both the molecular stacking within the single nanotube and packing of the nanotubes<sup>73</sup>.

Nanomaterials with well-defined pores have attracted considerable interest owing to their potential application in highly selective membranes. One simple yet effective strategy is the self-assembly of small molecules to generate well-ordered pores with precisely controlled size. Cyclic peptides can also be used for this purpose because of their capability to self-assemble into uniform nanotubes that can be easily modulated by tuning the number and type of amino acid residues. Sierra and co-workers prepared a porous liquid crystal with an internal diameter of 7 Å based on mesogenic dendron-conjugated cyclic peptide (cyclo-[D-S(Dn3)-(1*R*,3*S*)-MeN-γ-Acp-]<sub>3</sub>) self-assembly<sup>74</sup>. Both single and double channels could be achieved by altering the alkyl chain number within the mesogens.

There is an urgent and increasing demand for functional materials that resemble the multiscale architectures achieved by hierarchical self-assembly in nature. Controlled supramolecular self-assembly of synthetic building blocks in confined spaces can shed light on the fundamental mechanisms underlying the more complex behaviour of encapsulated polymer networks, but this still remains a challenge. To address this challenge, cyclic peptide nanotubes have been investigated as optimal building blocks for tunable preparation of fibrillary networks confined in water droplets. Three pH-sensitive amino acid residues (two H and one K) were included in the selected cyclic peptide building block. Therefore, the diameter and external chemical properties of the cyclic peptides tubes could be precisely modulated through pH-triggered supramolecular polymerization. An essential requirement for this study was the design of pH-sensitive synthetic cyclic peptides that could assemble into 1D nanostructures. The 1D hierarchical organization was perfectly transferred from the nanostructure to the microstructure. This strategy allowed direct microscopy imaging of the fibrillation process within a droplet<sup>75</sup>.

Due to their rigid geometry and tunable chemistry, DL-cyclic peptides have emerged as a promising building block for the rational design of materials in the microscale and nanoscale that exhibit hierarchical structures. Amyloids have been traditionally recognized as the most robust peptide materials, showing remarkable mechanical strength in the range of 2–4 GPa because of their dense hydrogen bond networks and ordered structure<sup>76</sup>. Displaying similar characteristics to amyloid fibrils, DL-cyclic peptides can facilitate the formation of high-aspect-ratio assemblies through β-sheet-like hydrogen bonding interactions<sup>77</sup>. For instance, assemblies of cyclo-([Q-D-L]<sub>4</sub>) (QL4) were found to be the stiffest and strongest among the known self-assembling peptide materials. It was found that hydrophobic effects guide the hierarchical organization of individual QL4 tubes into large rod-like assemblies in aqueous media<sup>78</sup> (FIG. 4d). Teixobactin, an 11-residue macrocyclic depsipeptide, has provided an efficient approach to treat antibiotic-resistant Gram-positive pathogens<sup>79</sup>. Previous findings revealed that the supramolecular assembly of teixobactin is associated with its antibiotic activity<sup>80</sup>. More recently, the X-ray crystallographic structure of an antibiotic teixobactin derivative revealed that the binding sites for oxyanions are formed as a result of the

organization into antiparallel  $\beta$ -sheets<sup>81</sup>. A lysine-containing teixobactin derivative (K<sub>10</sub>-teixobactin) was found to form amyloid-like fibrils and TEM images revealed the formation of multiple fibrils 100–200 nm in diameter consisting of oriented bundles of filaments with a cross-section of ~8 nm (REF.<sup>81</sup>).

### Amphiphilic peptides

Amphiphilic peptides have been designed to form various self-assembled nanostructures under different kinetic conditions ranging from nanofibres and nanobelts to nanoribbons<sup>82,83</sup>. Stupp and co-workers demonstrated that supramolecular self-assembly of such peptides could generate long nanofibres in aqueous solution<sup>83</sup>. Such 1D nanostructures have been reported to form crystalline bundles driven by repulsion forces rather than attractive interactions. A prominent study on amphiphilic peptide demonstrated the formation of a fibrillar network of Ala<sub>6</sub>Glu<sub>3</sub> (A6E3) stabilized by electrostatic repulsion between charged fibres<sup>11</sup> (FIG. 5a). Interestingly, additional charges resulting from the reversible ionization of –COOH groups induced by X-ray irradiation enabled the formation of fibre bundles also at the low amphiphilic peptide concentrations (5–10 mM), indicating that the increased charge density on the peptide nanofibre surfaces is the main driving force for the formation of the fibre bundles. This has been further evidenced by the similar bundling and orientation in other amphiphilic peptides with distinct sequences (such as VVAEEGGREDKQTV, VVAEEGGTKREEVD and AAEEGGREDKQTV) and the cytoskeleton of cells<sup>4</sup>. Moreover, such filament bundles trapped in a network were responsible for the subsequent crystallization<sup>11</sup>.

In contrast to filament ordering driven by repulsion forces, several hierarchical self-assembly ordered structures formed by attractions between neighbouring nanostructures have been reported. Tong and co-workers presented a pH-controlled hierarchical self-assembly of amphiphilic peptide with complementary attracting designer sequence including arginine and aspartic acid<sup>84</sup> (FIG. 5b). They found that the lateral association of nanofibres resulted in higher-order assemblies mediated by the complementary amino acid sequences with opposite charge. The charge of individual amino acids is pH dependent, therefore, tuning the solution pH enabled generation of surfaces with alternating positive and negative charges, providing control over the strength of interaction between the nanofibres.

By contrast, lateral assembly of nanofibres could not be obtained for those surfaces that did not exhibit altering charges. This study based on pH-modulated self-assembly provides insights into the fabrication of hierarchical supramolecular assemblies in a kinetically controlled manner.

With the development of peptide self-assembling nanostructures for potential biomedical applications, precise control over dimensions and shapes has become a central requirement. To this purpose, an amphiphilic peptide with an alternating hydrophobic–hydrophilic peptide sequence that can self-assemble into flat and wide nanobelts (FIG. 5c) has been proposed<sup>85</sup>. Further investigation of the nanobelt formation mechanism revealed that they form a grooved structure at high pH (in the presence of 2 mM NaOH) due to electrostatic repulsion. More interestingly, the lateral adhesion of  $\beta$ -sheets was also found to be dependent on the monomer concentration. An obvious morphology transformation from a flat nanobelt

into twisted nanoribbons was observed upon the decrease of the monomer concentration from 0.1 wt% to 0.01 wt%. Nyrkova and co-workers proposed a model in which the number of stacked layers was determined by thermodynamic and kinetic factors, such as peptide concentration or the intermolecular interactions between the peptide side chains, and observed that twisted linear structures could be formed through the lateral association of multiple twisted  $\beta$ -sheets<sup>86</sup>.

In addition to the kinetically controlled hierarchical self-assembly (such as concentration-modulated self-assembly), thermodynamically controlled self-assembly based on molecular structure design was also shown to be an effective strategy to control the dimensions and shapes of the nanostructures. The Bola-like amphiphilic peptides  $XI_4X$  ( $X$ =hydrophilic amino acid residues) are considered an excellent model to investigate the effect of hydrophilic amino acid substitutions on the morphology of the assembled structures. These  $XI_4X$  amphiphilic peptides have a tendency to form laterally associated  $\beta$ -sheets due to their symmetric molecular geometries and strong intermolecular interactions, including hydrophobic and hydrogen bonding<sup>87,88</sup>. Specifically,  $RI_4R$  mostly generates twisted and bilayered nanoribbons because of the high wetting degree and limited stacking of the  $\beta$ -sheet. By contrast,  $HI_4H$  mostly generates flat and multilayered nanoribbons because of their reduced wetting degree and substantial  $\beta$ -sheet stacking. This difference was suggested to arise from the residue pairing ( $R-R$  versus  $H-H$ ); for example, the hydrogen bonding motif between  $H$  residues contributes to the stacking of  $\beta$ -sheet monolayers along the  $c$  axis. Whereas lateral association of  $\beta$ -sheets may be preferred for self-assembly in the presence of  $KK$  pairings<sup>87</sup>, the formation of long nanotubes with large diameter was observed as a result of lateral stacking of  $KI_4K$   $\beta$ -sheets<sup>88</sup>. More recently, Xu and co-workers discovered that polar zippers between peptide  $\beta$ -sheets can self-organize into higher-ordered ribbons through intermeshing of many  $\beta$ -sheets due to the inherent directionality of hydrogen bonds<sup>89</sup>. Overall, these studies provide a paradigm for the modulation of hierarchical self-assembly from the perspective of molecular design. Similarly, amphiphilic lipid-mimicking decapeptides were designed, in which a phosphorylated serine head, two hydrophobic tails and an  $FF$  motif were included to facilitate the self-assembly and improve the nanostructure stability<sup>90</sup>. Such phosphopeptides have been shown to assemble into distinctive supramolecular nanostructures and undergo morphology evolution from sphere to fibrils and, finally, to half-elliptical nanosheets or curved nanotapes<sup>90</sup>. X-ray scattering and crystal structure analyses of such phosphopeptide nanosheets revealed the formation of a hierarchically oriented organization of fibres, which is stabilized by multiple hydrogen bonding and aromatic interactions<sup>91</sup>. Such a crystal structure of a two-tailed phosphopeptide demonstrated similarities to the natural phospholipid bilayer, the major component of cell membranes, indicating that more intricate yet ordered nanostructures with various biological and non-biological applications can be designed and prepared through molecular biomimicry.

Another representative study was conducted on a series of amphiphilic peptides containing dimeric repeats of valine–glutamic acid ( $VE$ )<sup>92</sup>, which are known to facilitate the formation of belt-like flat structures<sup>85</sup>. It was demonstrated that the lateral association of the primary structures could be tuned by varying the number of dimeric repeats (FIG. 5d). Long nanobelts of both  $(VE)_2$  and  $(VE)_4$  were obtained, the width of which could be modulated

by changing the pH and, consequently, their charge density. The thickness of the observed structures was mostly larger than that of a single bilayer, indicating oriented stacking of multiple nanostructures<sup>92</sup>.

The examples discussed above show that amphiphilic peptides are excellent building blocks to fabricate materials exhibiting multiscale organization. Amphiphilic peptides can be reversibly assembled and disassembled due to their highly dynamic nature, which makes them amenable to ordered alignment under external fields. It has been reported that amphiphilic peptide assemblies can be aligned under an external magnetic field, as confirmed by the change of the optical properties of material<sup>93</sup>. Furthermore, nematic alignment of the nanotubes formed by the Bola-amphiphilic arginine-capped peptide RFL<sub>4</sub>RF have been obtained at sufficiently high shear rates<sup>94</sup>.

In view of the capability of amphiphilic peptides to self-assemble into biocompatible hierarchical nanostructures, a bottom-up approach has been envisioned to produce stimuli-responsive molecular systems based on artificial peptide self-assembly. For example, an azobenzene-conjugated dipeptide amphiphile was found to form self-assembling nanoribbons<sup>95</sup>. Such nanoribbons formed from the alignment of the nanofibres in a lamellar manner, which is most likely driven by multiple non-covalent interactions, including directional forces (such as hydrogen bonding and ordered aromatic packing) and non-specific hydrophobic effects. Furthermore, a reversible transition between laminated nanoribbons and short fibres could be achieved under alternating UV and visible light irradiation<sup>95</sup>. Such peptide nanostructures with oriented organization provide a promising platform to mimic the dynamic self-assembly taking place in nature.

Peptide hydrogels containing charged amino acid residues, especially those with positive charge, may inevitably give rise to side effects, such as protein absorption in vitro. To address this issue, a series of non-ionic amphiphilic peptides which can readily self-assemble into clear hydrogels and are not susceptible to various media conditions, such as pH and ion strength, was synthesized<sup>96</sup>. Mechanistic study of the hydrogel formation revealed that these non-ionic amphiphilic peptide hydrogels exhibited fibril-like structures, such as nanofibres, helical ribbons, grooved nanobelts and twisted ribbons. It should be noted that the twisted ribbons or nanobelts consisted of several nanofibres organized side by side, held together by hydrogen bonds between the peripheral hydroxyl groups<sup>96</sup>.

From the perspective of intermolecular interactions, the hydrophilic–hydrophobic balance is crucial to the occurrence of hierarchically oriented organization. For example, the hydrophilic peptide sequence A $\beta$ (11–17) generally does not form characteristic amyloid fibrils owing to the absence of sufficient hydrophobic sequences. By contrast, such an A $\beta$  fragment with a long alkyl chain gives rise to distinct self-assemblies such as fibrils, fibril bundles and twisted ribbons under different conditions<sup>97</sup>. Specifically, tape-like fibril bundles are formed through lateral association of the parallel packed fibrils at a concentration of 1.87 mM at pH 3 (REF.<sup>97</sup>). By contrast, the FFKLVFF peptide based on A $\beta$ (16–20) is highly hydrophobic and forms self-assembling fibrils in polar organic solvent (such as methanol) at a low concentration. After conjugation with a hydrophilic polymer chain, polyethylene glycol, the resultant amphiphilic peptide exhibits

pronounced concentration-dependent selfassembly behaviour ranging from nematic to hexagonal columnar ordered structures<sup>98</sup>.

Unlike traditional amphiphilic peptides, nucleobase amphiphilic peptides are a novel type of peptide material that integrate multiple advantages of nucleosides, peptides and amphiphilic chemistry<sup>99,100</sup>. Such molecules possess robust and precise base-pairing interactions, which is beneficial for the hierarchical self-assembly. We have demonstrated that oriented GC dipeptide nucleic acid crystals can be formed and stabilized by stacking interaction and precise base-pairing interactions<sup>101</sup>. Furthermore, pronounced hierarchical self-assembly of nucleobase amphiphilic peptides based on a bi-tyrosine dipeptide has been reported. For such a system, rodlike or helical micelles could be initially formed, which would further self-assemble into nanoribbons under lateral or longitudinal hierarchical growth regimes<sup>102</sup>.

## Polypeptides

Considering the ubiquitous hierarchical self-assembly in nature, the core polypeptides derived from proteins have been explored as promising building blocks for the study of protein self-assembly, comprising a simpler model system for understanding protein architectures in functional and aberrant biology. Novel bio-inspired configurations exhibiting the structural and functional characteristics of naturally occurring architectures, or even new functionalities, have been investigated. Prime examples based on this strategy have focused on the formation of amyloid-like assemblies of peptide sequences containing the core recognition units of amyloidogenic proteins. A Tau protein-based 26-mer polypeptide fragment has been shown to form laminated amyloid ribbons through lateral assembly of protofilaments<sup>103</sup> (FIG. 6a). Similarly, inspired by the intermediate filaments and collagen-like assemblies, superhelical and coiled-coil fibres were obtained through the self-assembly of heptad repeats (H<sub>2</sub>N-SAib-F-S-Aib-F-Aib-OH, Aib = 2-aminoisobutyric acid) containing the characteristic collagen core sequence<sup>104</sup>. Although much effort has been devoted to investigating common biomimetic protein polymers, the in vitro self-assembly of peptides derived from other biopolymeric nanofibres, such as the bacterial type IV pilus (T4P), remains a challenge. To address this issue, a pilin-based 20-mer polypeptide building block derived from the *Geobacter sulfurreducens* pilin was designed based on the reductionist approach<sup>105</sup> (FIG. 6b). This polypeptide, consisting of the polymerization domain and functionality region of pilin, has been shown to self-assemble into ordered nanofibres. Densely packed fibre bundles were generated at a low polypeptide concentration, whereas a smooth and homogeneous layer of nanofibres was formed at a high concentration. This study may advance the design and development of other T4P-derived building blocks for biomimetic nanomaterials with specific functions found in other pilins through conjugation with a pilin-derived self-assembling peptide sequence.

In addition to protein-derived polypeptide selfassembly, de novo design of polypeptide self-assembly is a promising direction towards mechanistic understanding of protein multiscale architectures. Efforts have been devoted to unravelling the design rules of simple biomimetic polymer systems. As a class of peptidomimetics, polypeptoids have the advantages of sequence specificity typical of biomolecules and synthetic flexibility typical of traditional polymers due to their side chains appended to the peptide backbone<sup>106</sup>. In this context,

a bio-inspired peptoid diblock copolymer was designed and its aqueous self-assembly was investigated<sup>107</sup>. Monodispersed polypeptoid superhelices were formed through a hierarchical self-assembly process and, dependent on the molecule level of charge, X-ray scattering demonstrated the internal organization of the hierarchical assemblies, supporting the self-assembly model and the important role of intermolecular interactions, especially hydrogen bonds and electrostatic interactions, in the self-assembly process<sup>107</sup> (FIG. 6c).

In addition to charge interactions, the peptide sequence is another crucial factor that influences the final morphology<sup>108,109</sup>. A synthetic polypeptide has been de novo designed to form  $\beta$ -sheet filaments, which could further self-assemble into flat fibril laminates through lateral association<sup>109</sup> (FIG. 6d). The height of each fibril is equal to the extended length of the peptide monomer. Moreover, the lamination degree of the fibrils could be controlled by modulating the self-assembly kinetics factors, such as pH and temperature.

### Peptide-containing co-assembly systems

Multicomponent self-assembly is an emerging strategy to fabricate hierarchical architectures from simple biomolecules. Although still challenging, this approach can help enhance the complexity, such as long-range order and alignment across different scales, and functionality of a material<sup>110–112</sup>. We obtained highly ordered organization and subsequent long-range alignment in a co-assembly system of negatively-charged porphyrin and positively-charged KK dipeptide<sup>113</sup> (FIG. 7a). Nanorod-shaped J-aggregates were formed, stabilized mostly by strong  $\pi$ - $\pi$  stacking interactions of porphyrins. Such aggregates spontaneously aligned into fibre bundles, which are stabilized by a balance between van der Waals attraction and electrostatic repulsion. The long-range order in this hierarchical multiscale organization endows the fibre bundles with new properties, such as large Stokes shift and sustainable photocatalytic activity, which can be exploited for the growth of platinum nanowires<sup>113</sup>.

Oriented organization has also been applied for the co-assembly of peptide hydrogels. For example, Ulijn and co-workers reported the design and preparation of a hydrogel based on the co-assembly of Fmoc-FF and Fmoc-RGD<sup>114</sup>. AFM images revealed that numerous bundled and entangled nanofibres were formed. Detailed analysis of the morphology of individual nanofibers revealed that, for Fmoc-RGD 30 M%, co-assembled nanofibres formed highly ordered flat ribbons (FIG. 7b), as also demonstrated by the regular, periodic spacing between the diffraction peaks. Such a co-assembled hydrogel could be used as a 3D cell scaffold and was found to facilitate adhesion of dermal fibroblasts due to the specific RGD-integrin binding, followed by cell proliferation in vitro<sup>114</sup>. Similar hierarchical organization was also observed in a two-component self-assembly system containing Fmoc-FF and benzoate. In this case, nanobelts assembled from benzoate and formed hierarchically oriented nanosheets guided by the dynamic growth of a fibrous scaffold formed from the assembly of Fmoc-FF monomers<sup>115</sup>.

Inspired by the complex and elaborate hierarchically ordered structures found in nature, 3D materials with enhanced complexity, dynamic properties and diverse functionalities can be fabricated through dynamic self-assembly by controlling the molecular interactions between bioinspired molecules. A notable example is the construction of a dynamic system through the co-assembly of an elastin-like polypeptide and amphiphilic peptides<sup>116</sup>. This co-



assembled system yielded a robust membrane exhibiting multilayered architectures, which further evolved into tubular structures through a simultaneous spatiotemporal control that could serve as a bioactive tubular scaffold in tissue engineering<sup>116</sup> (FIG. 7c).

Peptide–DNA self-assembling is another emerging approach to generate multiscale hierarchical hybrid biomaterials<sup>117,118</sup>. Conticello and co-workers showed that co-assembly of collagen-mimetic peptides and DNA origami enabled the formation of nanowires with periodical separations of ~10 nm corresponding to the inter-sheet distances within the nanowires. Structurally ordered nanowires were generated through facial packing of DNA nanosheets (FIG. 7d). Moreover, the spacing between DNA nanosheets could be modulated by changing the central block of the peptide. Such cooperative effects of two types of biomolecules with different chemical structures and physical properties facilitate the development of bioelectronics and medical devices<sup>118</sup>.

Control of the topological morphologies and dimensions of the self-assembled aggregates is crucial to achieve versatile and realistic functions. Zhao and co-workers showed that Fmoc-modified amino acids can co-assemble into diverse complex superstructures with melamine following different transformation pathways (1D growth or 3D growth). Experimental observations revealed that the molecular organization modes and preferred fibre growth directions substantially influenced the transformation pathway complexity. Specifically, lamellar packing favoured 3D growth, whereas columnar packing favoured 1D growth. This study shed light on the fundamental relationship between molecular organization modes and the assemblies' morphology, thus providing general rules for the construction of co-assembled microstructures and nanostructures with desired functions<sup>119</sup>. Feng's group reported that the handedness of helical nanofibres can also be controlled by achiral additives, as shown in a study of a hydrogels composed of phenylalanine-based gelator and achiral bis(pyridinyl) derivatives. It was found that it is possible to change the handedness and arrangement orientation of the helical nanofibres by tuning the building block stoichiometry<sup>120</sup>. Further investigations on the regulation of the helicity and orientation of nanostructures have been conducted by Feng and colleagues by looking at the co-assembly of amino acid or short peptide derivatives with other components, such as bipyridine derivatives and metal ions. It appeared that the helicity and orientation of nanostructures could be modulated by the stoichiometry of additives as well as the type of metal ions<sup>121–123</sup>.

Recently, co-assembly has been used as an effective strategy to obtain long-range alignment of nanostructures. A seminal example is the co-assembly of single amphiphilic peptides (SAPs) and gemini-like amphiphilic peptides (GAPs)<sup>124</sup>. SAP-12 self-assembles into long fine fibres about 2–3 nm in diameter and several micrometres in length. When mixed with GAP-12 (GAP-12:SAP-12 = 1:3), rod-like short fibres about 7–8 nm in diameter and hundreds of nanometres in length are formed (FIG. 7e). Intriguingly, when the GAP-12 content is increased (to GAP-12:SAP-12 = 1:1), a spontaneous transformation from disorder to order — from random distribution to parallel-aligned 2D knitted fibrous arrays — was observed over time<sup>124</sup>. Soft natural structures, such as proteins, can reversibly self-assemble into functional architectures in a hierarchically oriented manner by virtue of non-covalent interactions. A recent relevant example demonstrated the molecular encoding

of such dynamic capabilities in co-assembly systems comprising peptide–DNA or DNA–mimetic peptide conjugates through the introduction of molecules or modulation of the charge density. Large-scale molecular arrangements resulting from non-covalent interactions facilitated this dynamic response<sup>125</sup>.

### Other organic molecules

In addition to the crystallization of short peptides and amino acids, macromolecular crystallization plays an important role in the fields of biological and materials science. Biopolymer crystallization has been conventionally considered to follow the classical crystallization theory<sup>42</sup>. However, a different biopolymer crystallization pathway was discovered to take place through mesoscale self-assembly of nanocrystals<sup>126</sup> (FIG. 8a). Core–shell protein nanocrystals were initially generated, which then further interacted with each other through the flexible shell. As a result, a protein mesocrystal formed through high-order self-assembly and oriented aggregation at a low biopolymer concentration, considerably lower than that required for classical nucleation. Such crystallization resulted in the formation of lamellae with high crystallinity yet unprecedented flexibility. This finding not only provides a novel perspective for the generation of flexible biopolymer assemblies with excellent crystallinity, but also provides an additional biopolymer crystallization mechanism for the advance of supra-molecular chemistry and nanoscience. In fact, oriented lateral growth is also observed in the self-assembly of other fibril-forming proteins (for example, hydrolysed lysozyme and  $\beta$ -lactoglobulin), peptidomimetic and protein-mimetic complexes, and even protein glucose isomerase<sup>127–130</sup>. For example, multiple morphologies, including lamellae, helical tubes and rhombic dodecahedra, were obtained through hierarchically oriented self-assembly of cyclodextrin–SDS complexes<sup>129</sup> (FIG. 8b).

In addition to proteins and peptides, small organic molecules, such as functional dyes, can also follow the principle of hierarchically oriented organization and form assembled microcrystals and nanocrystals. Perylene bisimides (PBIs) are a group of dyes of particular interest because of their distinguished advantages, including excellent chemical and photostability, strong visible light absorption and high fluorescence quantum yield<sup>131</sup>. Because of their strong intermolecular interactions in water due to a pronounced hydrophobic effect, amphiphilic PBI dyes appear to be the best-suited building blocks for hierarchical self-assembly in aqueous media<sup>131,132</sup>. In fact, robust PBI assemblies exhibiting long-range ordered structures in water are more easily achieved than assemblies of smaller and more flexible amphiphilic  $\pi$ -scaffolds held together by weak non-covalent interactions. Würthner and colleagues have investigated the growth process of PBI using TEM, cryo-TEM and AFM<sup>133</sup> (FIG. 8c). In this study, the hierarchical assembly of planar PBI in water was found to be concentration-dependent. Well-defined nanorods were obtained at a concentration of 0.05 mM, whereas thicker nanostructures were generated through the side-to-side arrangement of the nanorods at an increased concentration of 0.16 mM. Such thicker nanostructures could be divided into thinner ones in a side-to-side fission process. Notably, the nanorod fusion and fission process was reversible, as all of the intermediate morphologies could be found under the same sample conditions. Further increasing the sample concentration to two specific high concentrations (0.48 mM and 0.63

mM), single-layer nanoribbons 20–60 nm in width were generated through the oriented organization of nanorods. A similar self-assembly mechanism was also observed for the co-assembly of planar and core-twisted PBIs into liquid-crystalline materials for technological applications<sup>134</sup>. In this regard, Percec and co-workers have performed a series of studies to obtain liquid-crystalline columnar assemblies through chemical modifications of PBIs with different dendrons at the imide position that facilitated  $\pi$ – $\pi$  stacking interactions between chromophores<sup>135–138</sup>. Distinct from the above strategy, Würthner and colleagues showed that columnar singlestranded and multistranded J-aggregates in the liquidcrystalline phase could be obtained through the formation of hydrogen bonding and/or slipped  $\pi$ – $\pi$  stacking interactions in a series of tetra-bay phenoxy-dendronized PBIs<sup>139</sup>. Additionally, extremely long PBI nanofibres and hierarchically structured microfibrils consisting of ‘single stack’ PBI and quaterthiophene nanowires were also generated through the oriented organization mechanism<sup>140,141</sup>.

Self-assembly of amphiphilic molecules with a permanent charge (non-ionizable) consisting of azobenzene and a quaternary ammonium bromide terminal, with the aromatic groups playing a similar role to that of hydrogen bonds in other peptides, was also investigated, in which the nanofibres with high surface charge density were formed<sup>142</sup>. The fibre packing patterns and the underlying mechanism were investigated using smallangle X-ray scattering. Crystalline arrays were found to be formed through oriented alignment of the primary fibres 5.6 nm in diameter and separated 130 nm from each other. The packing mode and inter-fibre spacing could be modulated by changing the temperature or monomer concentration, whereas the hierarchical structures could be disassembled by the introduction of salt, thus revealing the essential role of electrostatic repulsions in the long-range organization. Such crystalline lattices of nanofibres could serve as a template for the preparation of organic–inorganic hybrid materials that could efficiently separate excitons for energy applications. In the context of the supramolecular nature and role of electrostatics in artificial systems, this study potentially provides further insights into the formation mechanism of cytoskeleton filaments exhibiting crystalline bundles<sup>142</sup>.

Also, hydrophobic dyes, such as Oil Red and Oil Blue, were shown to comply with crystallization pathways similar to those of amphiphilic molecules. Well-defined structures with high crystallinity were formed from miniemulsion nanodroplets through oriented aggregation of colloidal intermediates. In addition, to confirm that hydrophobic dyes can also follow the oriented organization crystallization pathway, this work unravels the essential role of ‘super-van der Waals’ forces between the single nanocrystals in the crystallization process<sup>143</sup>.

Porphyrins, some of the most outstanding functional dyes with  $\pi$ -conjugated chromophores, have received considerable attention for the generation of soft materials based on supramolecular self-assembly<sup>144</sup>. One of the most important merits of porphyrin self-assembly is its strong propensity for hierarchical assembly. Both the in situ-formed and as-obtained nanostructures can evolve into higher-ordered mesostructures or even microstructures<sup>145–148</sup>. Hexagonal nanotubes of zinc meso-tetra (4-pyridyl) porphyrin (ZnTPyP) were formed through oriented organization of the primary flake aggregates. Furthermore, such porphyrin nanotubes of uniform size and structure can evolve into well-

defined 3D smectic architectures after solvent evaporation. Furthermore, a recent study reported the salt-modulated hierarchical organization of nanotubes into bundles<sup>148</sup>. It was found that exciton transport in porphyrin aggregates was enhanced in the nanotube bundles rather than in the individual nanotube.

Oriented organization was also found in a co-assembly system of organic small molecules. A simple yet typical example is provided by hexagonal crystalline nanobelts that evolved from the columns of complex co-assemblies of *p*-aminoazobenzene hydrochloride (AzoHCl) and sodium bis(2-ethylhexyl) sulfosuccinate (AOT)<sup>149</sup>.

The fullerene molecule has also attracted much attention due to excellent optoelectronic, catalytic and mechanical properties. The controlled construction of fullerene microstructures and nanostructures is crucial to their application in various devices. A similar hierarchically oriented organization mechanism has been found in the construction of different fullerene nanostructures including nanowires, nanorods nanotubes and nanospheres. Xu and co-workers reported the formation of fullerene mesocrystals evolved from oriented-stacked nanocrystals<sup>150</sup> (FIG. 8d). Over time, the mesocrystals further transformed into a compact single crystal, accompanied by phase transition from mixed face-centred cubic and triclinic phases to a pure face-centred cubic phase. This finding provides evidence for a non-classical crystallization mechanism underlying the formation of a fullerene single crystal. In addition to the 1D assemblies, Zhang and Takeuchi employed a porphyrin polymer to control the assembly morphologies of C<sub>60</sub> (from 1D rods to 2D sheets and to complex 3D architectures) by tuning the supramolecular interactions<sup>151</sup>. In particular, C<sub>60</sub> single-crystalline microspheres were fabricated through oriented organization of the face-centred cubic nanoplates. More interestingly, thermotropic liquid crystal materials based on 2D fullerene crystals have also been reported<sup>152</sup>. These liquid crystals were smectic and exhibited a long-range order of the fullerene moieties within the lamella. These liquid crystals are representative examples of supramolecular liquid crystals with hierarchical multiscale structures. First, dyad molecules self-assembled into 2D crystals, which further evolved into supramolecular liquid crystals through lamella packing of the 2D crystals. The principle presented here paves the way for the design and fabrication of other types of liquid-crystal assemblies through hierarchically oriented organization.

## Principles for oriented organization

The examples described above depict the peptide hierarchical self-assembly or crystallization resulting from hierarchically oriented organization of the primary assemblies (such as nanofibres) and can be considered particle-based self-assemblies. Oriented organization represents one important growth pathway for supra-molecular polymerization and crystallization regardless of whether the obtained assemblies are metastable or thermodynamically stable<sup>43,153</sup>. Based on the examples discussed so far, we propose general requirements to achieve hierarchically oriented organization. The first requisite is that the elementary building blocks for the formation of primary supramolecular nanostructures are amphiphilic with balanced solvophobic and solvophilic sections. A narrow size dispersion of the supramolecular nanostructures facilitates the geometric packing and, ultimately, the hierarchically oriented self-assembly. Furthermore, thermodynamics and kinetics of

the nucleation growth are crucial for the eventual formation of hierarchical crystalline structures. It has been suggested that a high local concentration induced by fast nucleation can facilitate the oriented alignment of the primary nanostructures, as suggested by the entropy maximization principle, further leading to the sub-sequent crystallization<sup>34,100</sup>. In order to understand the underlying molecular mechanisms and gain deeper insights into hierarchically oriented organization, we need to define a theoretical framework that generalizes the rules for such phenomena. In the following, we discuss two major aspects of the underlying mechanisms: the intermolecular interactions responsible for hierarchically oriented organization and the thermodynamics and kinetics of such a multiscale self-assembly process. Subsequently, by comparison of the classical growth mechanism of self-assembly and crystallization and the hierarchically oriented organization mechanism with the proposed theoretical framework, we conclude that the latter agrees with the multistep crystallization process of organic molecules.

### The role of intermolecular interactions

It is known that non-covalent interactions predominantly facilitate the hierarchical multiscale self-assembly, wherein each type of interaction plays a specific role during the self-assembly process<sup>154–156</sup> (FIG. 9). For example, directional hydrogen bonds guide the fibrillation process for the formation of nanofibres. van der Waals interactions or hydrophobic effects guide the further fibre–fibre interactions, which also largely depend on the solvent medium. For the formation of oriented crystals, it is generally considered that a greater number of long-range directional intermolecular interactions, such as hydrogen bonding or  $\pi$ – $\pi$  stacking, should be involved<sup>63,157,158</sup>. The formation of different nanostructures, such as nanofibres, nanoribbons and nanosheets, results from the balance between these non-covalent interactions. Other intermolecular interactions, such as solute–solute and solvent–solute interactions, determine the self-assembly pathway and structure stability, thus playing a crucial role in shaping the energy landscape and phase behaviour of peptide assemblies. The imbalance of competing interactions of solvent molecules with the attractive sites of the nanostructures influences the directional bonding of the solute molecules, resulting in anisotropic growth<sup>125,153,159</sup>, and the rebalance between fibre–fibre and fibre–solvent interactions resulting from the rational molecular design could effectively influence the lateral assembly of initially formed nanofibers. For example, through modifying the outer surface of a coiled-coil peptide, it is possible to change the fibrils' response to heat: fibrils stabilized by hydrogen bonds melt on heating, whereas those stabilized by hydrophobic effects are strengthened upon heating<sup>160</sup>. Therefore, understanding the nature of the different non-covalent interactions and taking full advantage of their interplays are essential to design novel nanostructures with desired functions based on peptide self-assembly.

**Electrostatic interactions**—Electrostatic interactions between charged moieties in biomolecules are notably strong yet susceptible to the solvent polarity, which is highly relevant for self-assembly in an aqueous environment<sup>161,162</sup>. Screening of electrostatic interactions in the highly polar water medium leads to decreased attractions between charged groups<sup>163</sup>. In addition, the direct interactions between water molecules and charged groups further weaken the attraction but enhance repulsion between the charged groups, resulting in the dissociation of many salts. Therefore, multivalent interactions among multiple-charged

groups should be designed to strengthen the attractive electrostatic interactions in water. By contrast, strong interactions may be found between charged groups embedded in a hydrophobic microenvironment due to the inhibition of their interaction with water.

**Hydrogen bonding interaction**—Hydrogen bonding interaction is an important and universal type of intermolecular interaction found in nature, especially in biological systems<sup>164</sup>. The stability of protein and polypeptide secondary structures (such as  $\alpha$ -helices and  $\beta$ -sheets) is maintained by hydrogen bonds between amino acid residues. Similar to electrostatic interactions, hydrogen bonds are also substantially weakened in water. Therefore, hydrogen bonds enhanced by hydrophobic shielding are usually required for aqueous supramolecular polymerization<sup>165</sup>. Furthermore, the specificity and directionality of hydrogen bonds enable the rational design of supramolecular polymers.

**van der Waals interactions and  $\pi$ – $\pi$  stacking**—van der Waals interactions, such as dipolar and London dispersion interactions, take place between uncharged moieties and usually provide the highest contribution to the binding energies between non-polar components<sup>166</sup>. As a special case of van der Waals interactions,  $\pi$ – $\pi$  stacking occurs between large  $\pi$ -conjugated surfaces, resulting in an overall stability of supramolecular polymers held together by non-covalent interactions. The exact nature of these interactions is still under debate<sup>167,168,1</sup> but the attraction between the electron-rich and electron-lean  $\pi$ -surfaces was found to play an essential role in  $\pi$ – $\pi$  stacking<sup>169</sup>.

**Hydrophobic effect**—The hydrophobic effect results from the reorganization of hydrogen bond networks that accommodate hydrophobic molecules, and is considered to be entropically driven<sup>170</sup>. In this context, when the hydrophobic solutes enter a polar solvent such as water, the overall number of hydrogen bonds between water molecules is maintained more or less intact, but water molecules arrange around non-polar groups, forming ice-like static water clusters of decreased mobility<sup>171</sup>. Because the loss of mobility is entropically unfavourable, the entropy is increased by faster dynamics and the hydration water molecules from the icy-like cluster are released into the bulk so that their fast dynamics is restored and entropy increased. Simultaneously, hydrophobic building blocks tend to aggregate. Indeed, numerous thermodynamic studies have demonstrated the entropy-driven hydrophobic effect for small hydrophobes, indicating that this effect normally dominates the early stage of supramolecular self-assembly in a polar medium.

## Thermodynamics and kinetics

Hierarchically oriented organization of peptide hierarchical self-assembly and crystallization is synergistically controlled by thermodynamics and kinetics. Therefore, we can analyse such processes from the point of view of energy and dynamics<sup>172</sup>. The interaction between the primary assemblies can be modulated by modifying the properties of the assemblies' surfaces and the solvent. Short-range repulsive interactions have been demonstrated to be predominant under certain conditions. In this case, entropy must be the driving force behind the rearrangement. The oriented organization of peptide self-assembling nanostructures must lead to entropy maximization of the whole system, because surface water or other solvent



molecules would be expelled from the primary self-assembling structures when the latter align in parallel to yield high-ordered assemblies.

The general rule that emerges from the examples of hierarchical self-assembly and oriented crystallization is that the entropic contribution to the ordering transformation is crucial to the design and development of self-assembling supramolecular materials with addressable complexity. Considering the short-range interactions between the primary assemblies, the principle of entropic ordering can be deduced by considering a geometrical perspective<sup>173</sup>. For example, at low concentrations, isotropic suspensions of rods are formed as a result of the dominating rotational entropy, whereas rod aggregates with a preferred direction are generated when the concentration is increased to a critical value due to their predominating packing entropy. Such a viewpoint provides insights into the effect of entropy on the structure of matter and the dynamic formation process. The classical theory description for this viewpoint agrees with Onsager's theory that clarifies the ordering influence of entropy. According to Onsager's argument, the entropy loss resulting from orientated ordering is more than compensated for by the entropy gain associated with the free volume increase in the orientated ordering state at sufficiently high concentrations<sup>174</sup>. This argument is based on the fact that parallel rods occupy less space than randomly oriented rods, thereby leaving more space for water molecules to move in (FIG. 10). This means that rods should align in parallel to maximize their freedom for translation at a high concentration. Therefore, the isotropic–nematic transition is of entropic origin. Onsager's theory also explains why bundles can be formed from colloid nanorods with the same charge, and also applies to the formation of bundles of both biological and non-biological fibres. Experimental data and theoretical predictions demonstrate the formation of bundles through saltbridge-like attractive forces between neighbouring filaments<sup>175</sup>. Different from the filament bundling induced by attractive forces, long-range electrostatic repulsion is also found to be crucial to direct the formation of stable filament bundles with wide spacing<sup>11</sup>. Ongoing theoretical research further unravels the mechanism underlying the crystallization of bundles in filament networks, showing that the interplay of filament–filament long-range repulsion and confinement potential give rise to the formation of the hexagonal crystalline order<sup>176</sup>.

### Comparison with the classical growth theory

Traditionally, supramolecular self-assembly and crystallization have been widely described by the classical monomer-by-monomer addition to an isolated cluster. Such a growth mechanism relies on the Ostwald ripening process, that is, the dissolution of small particles in favour of large particles over time, driven by the decrease of surface energy<sup>177</sup>. During this process, crystal growth is initiated by the formation of highly ordered nuclei in a supersaturated medium. Based on the Gibbs–Thompson law, an energy difference exists between the large and small particles, which results in the further growth of larger particles and the dissolution of the small particles<sup>178</sup>.

In contrast to the classical growth mechanism, hierarchically oriented organization is a particle-mediated growth mechanism that involves the oriented organized self-assembly of primary assemblies and their subsequent conversion into the highly ordered crystals. Such a process does not involve the dissolution of primary assemblies, which is distinct from the

Ostwald ripening process. The driving force for this spontaneous oriented organization is the entropy in the form of attractive depletion forces and entropic ordering forces. Evidence of oriented organization has been frequently observed in the high-order self-assembly and crystallization of various organic molecules in the above examples, such as amino acids, peptides and dyes, from initially homogeneous solutions. Such an oriented organization pathway would have important implications for the structure and function of materials, as oriented organization occurs at the particle interface generated during the aggregation process. This results in the production of anisotropic microstructures and nanostructures, nonequilibrium symmetries and distinct internal defects and element distributions. These characteristics would have dramatic influence on the structural stability and on features including optical properties, mechanical behaviour and catalytic activity of the resulting materials. Therefore, oriented organization enables the modulation of material properties by tuning the morphology, size and defect concentrations.

## Conclusions and outlook

This Review summarizes the hierarchically oriented organization principle, a newly proposed supramolecular architecture growth mechanism underlying the high-order self-assembly and crystallization of peptides and other small organic molecules. We analyse the multiscale hierarchical self-assembly process from the point of view of thermodynamics and kinetics, aiming to understand the underlying molecular interactions involved in the high-order self-assembly and crystallization process over multiple-length scales and to construct a theoretical framework to describe the hierarchically oriented organization mechanism. It has been found that biomoleculebased multifunctional materials with highly ordered structures can be achieved by hierarchical architectures with anisotropy. The realization of hierarchically oriented organization of peptide self-assembly is facilitated by rational control of weak intermolecular interactions governing the self-assembly process at different stages. Compared with the classical Ostwald ripening mechanism that suitably describes diffusion-controlled growth processes, the oriented organization mechanism is regulated by specific requirements that lead primary nanostructures to hierarchically orient into higher-order assemblies that cannot be otherwise nucleated through a classical growth mechanism.

Extensive supramolecular architectures of peptides and their derivatives have exemplified their hierarchically oriented organization, although in-depth understanding of fundamental mechanisms underlying the oriented organization process still remains elusive. For example, the role of solvent molecules including their types and local ordering in the oriented organization process still remains unclear. The physics and chemistry at the interface between the primary assemblies, which is crucial for their alignment and attachment, are as yet poorly understood. We speculate that a complete crystallization of perfect crystals must include the classical Ostwald ripening and monomer-by-monomer addition. Although numerous experimental results have demonstrated that assembly kinetics plays a crucial role in the hierarchical self-assembly and crystallization of different peptides, the quantitative consensus and the theoretical comprehension will be highly appreciated to elaborate the kinetics and the thermodynamic basis for the occurrence of oriented organization. Furthermore, understanding of the dynamics and driving forces of the movement and alignment of elementary nanostructures still remains challenging.

The primary challenge is the direct acquisition of experimental data during the highly dynamic, multiscale structural evolution that hinders the construction of assembly kinetic models. Furthermore, the study of the oriented organization mechanism mainly focuses on growth kinetics rules, driving forces and the accompanying phase transition, but it is a top priority to conduct systematic studies on the role of peptide sequence, length and relative contribution of different non-covalent interactions during the formation of peptide crystals and other supramolecular polymers.

From a long-term perspective, the more accurate and potent approaches for tracking the detailed dynamics of hierarchical self-assembly and crystallization process will be the combination of in situ imaging and structural analysis methods. In situ high-resolution imaging of assemblies can be a critical step towards the construction of appropriate and precise models describing oriented organization. This is a fundamental yet particularly challenging requirement for the characterization of assemblies in situ in a solution environment. Liquid cell in situ TEM allows us to elucidate the fundamental processes of hierarchical self-assembly and crystallization through quantitative analysis of the motions and dynamic interactions of particles in liquid media. Similar details about the morphology evolution can also be acquired using cryo-TEM, especially single-particle cryo-TEM, which is expected to enrich our understanding of the interactions between particles at the molecular level.

In addition to direct imaging of the assemblies, techniques that can offer reliable data for quantitative description of the thermodynamics and kinetics of oriented organization are of equal importance. Moreover, classical phase transition and colloidal theories may provide inspiration for the construction of a quantitative thermodynamic and kinetic framework. The latter will facilitate the establishment of thermodynamics and kinetics models enabling the description and understanding of the assembly mechanism, which is critical to the design of novel nanostructures and for modulating material properties and functions. In situ characterization of the driving forces involved in the oriented organization process is another key issue.

Although many critical challenges remain, we are strongly convinced that the oriented organization principle is at an exciting juncture to contribute to the development of advanced functional materials based on hierarchical self-assembly and crystallization.

## Acknowledgements

The authors acknowledge financial support from the National Natural Science Foundation of China (project nos 21522307, 21802143 and 21802144), the National Natural Science Fund BRICS STI Framework Programme (no. 51861145304) and Innovation Research Community Science Fund (no. 21821005), and the Key Research Program of Frontier Sciences of the Chinese Academy of Sciences (CAS, grant no. QYZDB-SSW-JSC034) as well as the European Research Council under the European Union Horizon 2020 research and innovation programme (BISON no. 694426). The authors thank Sigal Rencus-Lazar for language editing assistance.

## References

1. Knowles TPJ, Oppenheim TW, Buell AK, Chirgadze DY, Welland ME. Nanostructured films from hierarchical self-assembly of amyloidogenic proteins. *Nat Nanotechnol.* 2010; 5: 204–207. DOI: 10.1038/nnano.2010.26 [PubMed: 20190750]

2. Karsenti E. Self-organization in cell biology: a brief history. *Nat Rev Mol Cell Biol.* 2008; 9: 255–262. [PubMed: 18292780]
3. Yao H-B, Fang H-Y, Wang X-H, Yu S-H. Hierarchical assembly of micro-/nano-building blocks: bio-inspired rigid structural functional materials. *Chem Soc Rev.* 2011; 40: 3764–3785. [PubMed: 21431109]
4. Pelletier O, et al. Structure of actin cross-linked with  $\alpha$ -actinin: a network of bundles. *Phys Rev Lett.* 2003; 91: 148102. [PubMed: 14611558]
5. Gardel ML, et al. Elastic behavior of cross-linked and bundled actin networks. *Science.* 2004; 304: 1301–1305. [PubMed: 15166374]
6. Wong GCL, et al. Lamellar phase of stacked twodimensional rafts of actin filaments. *Phys Rev Lett.* 2003; 91: 018103. [PubMed: 12906579]
7. Adler-Abramovich L, et al. Bioinspired flexible and tough layered peptide crystals. *Adv Mater.* 2017; 30: 1704551. [PubMed: 29215205]
8. Tao K, Makam P, Aizen R, Gazit E. Selfassembling peptide semiconductors. *Science.* 2017; 358: eaam9756. doi: 10.1126/science.aam9756 [PubMed: 29146781]
9. Fitzpatrick AWP, et al. Atomic structure and hierarchical assembly of a cross- $\beta$  amyloid fibril. *Proc Natl Acad Sci USA.* 2013; 110: 5468–5473. DOI: 10.1073/pnas.1219476110 [PubMed: 23513222]
10. Bera S, Mondal S, Rencus-Lazar S, Gazit E. Organization of amino acids into layered supramolecular secondary structures. *Acc Chem Res.* 2018; 51: 2187–2197. DOI: 10.1021/acs.accounts.8b00131 [PubMed: 30095247]
11. Cui H, et al. Spontaneous and X-ray-triggered crystallization at long range in self-assembling filament networks. *Science.* 2010; 327: 555–559. DOI: 10.1126/science.1182340 [PubMed: 20019248]
12. Liu X, et al. Transformation of dipeptide-based organogels into chiral crystals by cryogenic treatment. *Angew Chem Int Ed.* 2017; 56: 2660–2663. [PubMed: 28140492]
13. Yan X, Li J, Möhwald H. Self-assembly of hexagonal peptide microtubes and their optical waveguiding. *Adv Mater.* 2011; 23: 2796–2801. [PubMed: 21495089]
14. Liu Y, et al. Self-assembled supramolecular nanotube yarn. *Adv Mater.* 2013; 25: 5875–5879. [PubMed: 23943418]
15. Reches M, Gazit E. Controlled patterning of aligned self-assembled peptide nanotubes. *Nat Nanotechnol.* 2006; 1: 195–200. [PubMed: 18654186]
16. Valéry C, et al. Biomimetic organization: octapeptide self-assembly into nanotubes of viral capsid-like dimension. *Proc Natl Acad Sci USA.* 2003; 100: 10258–10262. DOI: 10.1073/pnas.1730609100 [PubMed: 12930900]
17. Reches M, Gazit E. Casting metal nanowires within discrete self-assembled peptide nanotubes. *Science.* 2003; 300: 625–627. [PubMed: 12714741]
18. Li Q, Jia Y, Dai L, Yang Y, Li J. Controlled rod nanostructured assembly of diphenylalanine and their optical waveguide properties. *ACS Nano.* 2015; 9: 2689–2695. [PubMed: 25759013]
19. Kim J, et al. Role of water in directing diphenylalanine assembly into nanotubes and nanowires. *Adv Mater.* 2010; 22: 583–587. [PubMed: 20217753]
20. Yan X, et al. Transition of cationic dipeptide nanotubes into vesicles and oligonucleotide delivery. *Angew Chem Int Ed.* 2007; 46: 2431–2434. [PubMed: 17328086]
21. Wang Y, et al. Capillary force-driven, hierarchical co-assembly of dandelion-like peptide microstructures. *Small.* 2015; 11: 2893–2902. [PubMed: 25759325]
22. Su Y, et al. A peony-flower-like hierarchical mesocrystal formed by diphenylalanine. *J Mater Chem.* 2010; 20: 6734–6740.
23. Peterson DT, Baker HH, Verhoeven JD. Damascus steel, characterization of one damascus steel sword. *Mater Charact.* 1990; 24: 355–374.
24. Frederix PWJM, et al. Exploring the sequence space for (tri-)peptide self-assembly to design and discover new hydrogels. *Nat Chem.* 2014; 7: 30–37. [PubMed: 25515887]
25. Lampel A, et al. Polymeric peptide pigments with sequence-encoded properties. *Science.* 2017; 356: 1064–1068. [PubMed: 28596363]

26. Chan KH, Xue B, Robinson RC, Hauser CAE. Systematic moiety variations of ultrashort peptides produce profound effects on self-assembly, nanostructure formation, hydrogelation, and phase transition. *Sci Rep.* 2017; 7: 12897. doi: 10.1038/s41598-017-12694-9 [PubMed: 29018249]
27. Bortolini C, et al. Rapid growth of acetylated A $\beta$ (16-20) into macroscopic crystals. *ACS Nano.* 2018; 12: 5408–5416. [PubMed: 29771495]
28. Tang C, Ulijn RV, Saiani A. Effect of glycine substitution on Fmoc-diphenylalanine self-assembly and gelation properties. *Langmuir.* 2011; 27: 14438–14449. [PubMed: 21995651]
29. Ejgenberg M, Mastai Y. Hierarchical superstructures of l-glutathione. *Cryst Growth Des.* 2018; 18: 5063–5068.
30. Cenker ÇÇ, et al. Peptide nanotube formation: a crystal growth process. *Soft Matter.* 2012; 8: 7463–7470.
31. Lu K, Jacob J, Thiyagarajan P, Conticello VP, Lynn DG. Exploiting amyloid fibril lamination for nanotube self-assembly. *J Am Chem Soc.* 2003; 125: 6391–6393. [PubMed: 12785778]
32. Wang Y, et al. Columnar liquid crystals self-assembled by minimalistic peptides for chiral sensing and synthesis of ordered mesoporous silica. *Chem Mater.* 2018; 30: 7902–7911.
33. Schwahn D, Ma Y, Cölfen H. Mesocrystal to single crystal transformation of d,l-alanine evidenced by small angle neutron scattering. *J Phys Chem C.* 2007; 111: 3224–3227.
34. Medina DD, Mastai Y. Synthesis of DL-alanine mesocrystals with a hollow morphology. *Cryst Growth Des.* 2008; 8: 3646–3651.
35. Nemtsov I, Mastai Y, Ejgenberg M. Formation of hierarchical structures of l-glutamic acid with an l-arginine additive. *Cryst Growth Des.* 2018; 18: 4054–4059.
36. Ma Y, Cölfen H, Antonietti M. Morphosynthesis of alanine mesocrystals by pH control. *J Phys Chem B.* 2006; 110: 10822–10828. [PubMed: 16771332]
37. Ejgenberg M, Mastai Y. Biomimetic crystallization of l-cystine hierarchical structures. *Cryst Growth Des.* 2012; 12: 4995–5001.
38. Elemans JAAW, Lei S, De Feyter S. Molecular and supramolecular networks on surfaces: from two-dimensional crystal engineering to reactivity. *Angew Chem Int Ed.* 2009; 48: 7298–7332. [PubMed: 19746490]
39. Wang X-Y, Narita A, Müllen K. Precision synthesis versus bulk-scale fabrication of graphenes. *Nat Rev Chem.* 2017; 2: 0100.
40. Love JC, Estroff LA, Kriebel JK, Nuzzo RG, Whitesides GM. Self-assembled monolayers of thiolates on metals as a form of nanotechnology. *Chem Rev.* 2005; 105: 1103–1170. [PubMed: 15826011]
41. Chen J, et al. Building two-dimensional materials one row at a time: avoiding the nucleation barrier. *Science.* 2018; 362: 1135–1139. [PubMed: 30523105]
42. Kashchiev, D. *Nucleation: Basic Theory with Applications.* Butterworth Heinemann; 2000.
43. Liyanage W, Brennessel WW, Nilsson BL. Spontaneous transition of self-assembled hydrogel fibrils into crystalline microtubes enables a rational strategy to stabilize the hydrogel state. *Langmuir.* 2015; 31: 9933–9942. [PubMed: 26305488]
44. Rajbhandary A, Raymond DM, Nilsson BL. Selfassembly, hydrogelation, and nanotube formation by cation-modified phenylalanine derivatives. *Langmuir.* 2017; 33: 5803–5813. [PubMed: 28514156]
45. Liyanage W, Nilsson BL. Substituent effects on the self-assembly/coassembly and hydrogelation of phenylalanine derivatives. *Langmuir.* 2016; 32: 787–799. [PubMed: 26717444]
46. Rajbhandary A, Brennessel WW, Nilsson BL. Comparison of the self-assembly behavior of Fmoc-phenylalanine and corresponding peptoid derivatives. *Cryst Growth Des.* 2018; 18: 623–632.
47. Song J, et al. Crystalline dipeptide nanobelts based on solid-solid phase transformation self-assembly and their polarization imaging of cells. *ACS Appl Mater interfaces.* 2018; 10: 2368–2376. [PubMed: 29285927]
48. Pappas CG, et al. Alignment of nanostructured tripeptide gels by directional ultrasonication. *Chem Commun.* 2015; 51: 8465–8468. [PubMed: 25891849]
49. Lu Q, et al. Hydrogel assembly with hierarchical alignment by balancing electrostatic forces. *Adv Mater interfaces.* 2016; 3: 1500687.

50. Hill A, et al. Alignment of aromatic peptide tubes in strong magnetic fields. *Adv Mater.* 2007; 19: 4474–4479.
51. Zhang S, et al. A self-assembly pathway to aligned monodomain gels. *Nat Mater.* 2010; 9: 594–601. DOI: 10.1038/nmat2778 [PubMed: 20543836]
52. Zhan J, et al. Supramolecular silk from a peptide hydrogel. *Mater Chem Front.* 2017; 1: 911–915.
53. Wall BD, et al. Aligned macroscopic domains of optoelectronic nanostructures prepared via shear-flow assembly of peptide hydrogels. *Adv Mater.* 2011; 23: 5009–5014. [PubMed: 22180891]
54. Qin S-Y, Pei Y, Liu X-J, Zhuo R-X, Zhang X-Z. Hierarchical self-assembly of a  $\beta$ -amyloid peptide derivative. *J Mater Chem B.* 2013; 1: 668–675. [PubMed: 32260771]
55. Sun B, et al. Self-assembly of ultralong aligned dipeptide single crystals. *ACS Nano.* 2017; 11: 10489–10494. [PubMed: 28945958]
56. Hu Y, et al. Electrostatic-driven lamination and untwisting of  $\beta$ -sheet assemblies. *ACS Nano.* 2016; 10: 880–888. [PubMed: 26646791]
57. Wang M, Du L, Wu X, Xiong S, Chu PK. Charged diphenylalanine nanotubes and controlled hierarchical self-assembly. *ACS Nano.* 2011; 5: 4448–4454. [PubMed: 21591732]
58. Manchineella S, Govindaraju T. Molecular selfassembly of cyclic dipeptide derivatives and their applications. *ChemPlusChem.* 2016; 82: 88–106. [PubMed: 31961506]
59. Hu K, et al. Tuning peptide self-assembly by an in-tether chiral center. *Sci Adv.* 2018; 4: eaar5907. doi: 10.1126/sciadv.aar5907 [PubMed: 29756036]
60. Fears KP, et al. High-performance nanomaterials formed by rigid yet extensible cyclic  $\beta$ -peptide polymers. *Nat Commun.* 2018; 9: 4090. doi: 10.1038/s41467-018-06576-5 [PubMed: 30291243]
61. Ziganshin MA, et al. Thermally induced selfassembly and cyclization of l-leucyl-l-leucine in solid state. *J Phys Chem B.* 2017; 121: 8603–8610. [PubMed: 28820260]
62. Manchineella S, Govindaraju T. Hydrogen bond directed self-assembly of cyclic dipeptide derivatives: gelation and ordered hierarchical architectures. *RSCAdv.* 2012; 2: 5539–5542.
63. Yan X, Su Y, Li J, Früh J, Möhwald H. Uniaxially oriented peptide crystals for active optical waveguiding. *Angew Chem int Ed.* 2011; 50: 11186–11191. [PubMed: 21956859]
64. Li Y, et al. Solvothermally mediated self-assembly of ultralong peptide nanobelts capable of optical waveguiding. *Small.* 2016; 12: 2575–2579. [PubMed: 27028848]
65. Tao K, et al. Quantum confined peptide assemblies with tunable visible to near-infrared spectral range. *Nat Commun.* 2018; 9: 3217. doi: 10.1038/s41467-018-05568-9 [PubMed: 30104564]
66. Pianowski ZL, Karcher J, Schneider K. Photoresponsive self-healing supramolecular hydrogels for light-induced release of DNA and doxorubicin. *Chem Commun.* 2016; 52: 3143–3146. [PubMed: 26804160]
67. Barman AK, Verma S. Solid state structures and solution phase self-assembly of clicked mannosylated diketopiperazines. *RSC Adv.* 2013; 3: 14691–14700.
68. Seo MJ, et al. Reversibly thermochromic cyclic dipeptide nanotubes. *Langmuir.* 2018; 34: 8365–8373. [PubMed: 29933690]
69. Palacin S, et al. Hydrogen-bonded tapes based on symmetrically substituted diketopiperazines: a robust structural motif for the engineering of molecular solids. *J Am Chem Soc.* 1997; 119: 11807–11816.
70. Govindaraju T. Spontaneous self-assembly of aromatic cyclic dipeptide into fibre bundles with high thermal stability and propensity for gelation. *Supramol Chem.* 2011; 23: 759–767.
71. Jeziorna A, et al. Cyclic dipeptides as building units of nano- and microdevices: synthesis, properties, and structural studies. *Cryst Growth Des.* 2015; 15: 5138–5148.
72. Govindaraju T, Pandeewar M, Jayaramulu K, Jaipuria G, Atreya HS. Spontaneous self-assembly of designed cyclic dipeptide (Phg–Phg) into twodimensional nano- and mesosheets. *Supramol Chem.* 2011; 23: 487–492.
73. Leclair S, et al. Micrometer-sized hexagonal tubes self-assembled by a cyclic peptide in a liquid crystal. *Angew Chem int Ed.* 2004; 43: 349–353. [PubMed: 14705095]
74. Amornin M, et al. Liquid crystal organization of selfassembling cyclic peptides. *Chem Commun.* 2014; 50: 688–690. [PubMed: 24281818]



75. Méndez-Ardoy A, Granja JR, Montenegro J. pH-triggered self-assembly and hydrogelation of cyclic peptide nanotubes confined in water micro-droplets. *Nanoscale Horiz.* 2018; 3: 391–396. [PubMed: 32254126]
76. Smith JF, Knowles TPJ, Dobson CM, MacPhee CE, Welland ME. Characterization of the nanoscale properties of individual amyloid fibrils. *Proc Natl Acad Sci USA.* 2006; 103: 15806–15811. DOI: 10.1073/pnas.0604035103 [PubMed: 17038504]
77. Ghadiri MR, Granja JR, Milligan RA, McRee DE, Khazanovich N. Self-assembling organic nanotubes based on a cyclic peptide architecture. *Nature.* 1993; 366: 324–327. [PubMed: 8247126]
78. Rubin DJ, et al. Structural, nanomechanical, and computational characterization of d,l-cyclic peptide assemblies. *ACS Nano.* 2015; 9: 3360–3368. [PubMed: 25757883]
79. Ling LL, et al. A new antibiotic kills pathogens without detectable resistance. *Nature.* 2015; 517: 455–459. DOI: 10.1038/nature14098 [PubMed: 25561178]
80. Parmar A, et al. Defining the molecular structure of teixobactin analogues and understanding their role in antibacterial activities. *Chem Commun.* 2017; 53: 2016–2019. [PubMed: 28124045]
81. Yang H, Wierzbicki M, Du Bois DR, Nowick JS. X-ray crystallographic structure of a teixobactin derivative reveals amyloid-like assembly. *J Am Chem Soc.* 2018; 140: 14028–14032. DOI: 10.1021/jacs.8b07709 [PubMed: 30296063]
82. Cui H, Cheetham AG, Pashuck ET, Stupp SI. Amino acid sequence in constitutionally isomeric tetrapeptide amphiphiles dictates architecture of one-dimensional nanostructures. *J Am Chem Soc.* 2014; 136: 12461–12468. DOI: 10.1021/ja507051w [PubMed: 25144245]
83. Hartgerink JD, Beniash E, Stupp SI. Selfassembly and mineralization of peptide-amphiphile nanofibers. *Science.* 2001; 294: 1684–1688. [PubMed: 11721046]
84. Chen Y, Gan HX, Tong YW. pH-controlled hierarchical self-assembly of peptide amphiphile. *Macromolecules.* 2015; 48: 2647–2653.
85. Cui H, Muraoka T, Cheetham AG, Stupp SI. Self-assembly of giant peptide nanobelts. *Nano Lett.* 2009; 9: 945–951. DOI: 10.1021/nl802813f [PubMed: 19193022]
86. Aggeli A, et al. Hierarchical self-assembly of chiral rod-like molecules as a model for peptide  $\beta$ -sheet tapes, ribbons, fibrils, and fibers. *Proc Natl Acad Sci USA.* 2001; 98: 11857–11862. DOI: 10.1073/pnas.191250198 [PubMed: 11592996]
87. Zhao Y, et al. Tuning one-dimensional nanostructures of bola-like peptide amphiphiles by varying the hydrophilic amino acids. *Chem Eur J.* 2016; 22: 11394–11404. [PubMed: 27362441]
88. Zhao Y, et al. Controlling the diameters of nanotubes self-assembled from designed peptide bolaphiles. *Small.* 2018; 14: 1703216. [PubMed: 29430820]
89. Wang M, et al. Nanoribbons self-assembled from short peptides demonstrate the formation of polar zippers between  $\beta$ -sheets. *Nat Commun.* 2018; 9: 5118. doi: 10.1038/s41467-018-07583-2 [PubMed: 30504813]
90. Pellach M, et al. Spontaneous structural transition in phospholipid-inspired aromatic phosphopeptide nanostructures. *ACS Nano.* 2015; 9: 4085–4095. [PubMed: 25802000]
91. Pellach M, et al. A two-tailed phosphopeptide crystallizes to form a lamellar structure. *Angew Chem int Ed.* 2017; 56: 3252–3255. DOI: 10.1002/anie.201609877 [PubMed: 28191715]
92. Moyer TJ, Cui H, Stupp SI. Tuning nanostructure dimensions with supramolecular twisting. *J Phys Chem B.* 2013; 117: 4604–4610. DOI: 10.1021/jp3087978 [PubMed: 23145959]
93. Löwik DWPM, et al. A highly ordered material from magnetically aligned peptide amphiphile nanofiber assemblies. *Adv Mater.* 2007; 19: 1191–1195.
94. Hamley IW, et al. Shear alignment of bola-amphiphilic arginine-coated peptide nanotubes. *Biomacromolecules.* 2017; 18: 141–149. [PubMed: 27983808]
95. Lin Y, Qiao Y, Tang P, Li Z, Huang J. Controllable self-assembled laminated nanoribbons from dipeptide-amphiphile bearing azobenzene moiety. *Soft Matter.* 2011; 7: 2762–2769.
96. Wan Y, Wang Z, Sun J, Li Z. Extremely stable supramolecular hydrogels assembled from nonionic peptide amphiphiles. *Langmuir.* 2016; 32: 7512–7518. [PubMed: 27399915]
97. Deng M, Yu D, Hou Y, Wang Y. Self-assembly of peptide-amphiphile C12-A $\beta$ (11–17) into nanofibrils. *J Phys Chem B.* 2009; 113: 8539–8544. [PubMed: 19534562]

98. Hamley IW, et al. Nematic and columnar ordering of a PEG-peptide conjugate in aqueous solution. *Chem Eur J.* 2008; 14: 11369–11375. [PubMed: 18618539]
99. Guler MO, Pokorski JK, Appella DH, Stupp SI. Enhanced oligonucleotide binding to self-assembled nanofibers. *Bioconjugate Chem.* 2005; 16: 501–503. [PubMed: 15898715]
100. Ura Y, Beierle JM, Leman LJ, Orgel LE, Ghadiri MR. Self-assembling sequence-adaptive peptide nucleic acids. *Science.* 2009; 325: 73–77. [PubMed: 19520909]
101. Berger O, et al. Light-emitting self-assembled peptide nucleic acids exhibit both stacking interactions and Watson–Crick base pairing. *Nat Nanotechnol.* 2015; 10: 353. [PubMed: 25775151]
102. Serpell CJ, et al. Nucleobase peptide amphiphiles. *Mater Horiz.* 2014; 1: 348–354.
103. Adamcik J, et al. Microtubule-binding R3 fragment from Tau self-assembles into giant multistranded amyloid ribbons. *Angew Chem Int Ed.* 2016; 55: 618–622. [PubMed: 26636567]
104. Mondal S, et al. Formation of functional super-helical assemblies by constrained single heptad repeat. *Nat Commun.* 2015; 6: 8615. doi: 10.1038/ncomms9615 [PubMed: 26468599]
105. Guterman T, et al. Formation of bacterial pilus-like nanofibres by designed minimalistic self-assembling peptides. *Nat Commun.* 2016; 7: 13482. doi: 10.1038/ncomms13482 [PubMed: 27853136]
106. Gangloff N, Ulbricht J, Lorson T, Schlaad H, Luxenhofer R. Peptoids and polypeptoids at the frontier of supra- and macromolecular engineering. *Chem Rev.* 2016; 116: 1753–1802. [PubMed: 26699377]
107. Murnen HK, Rosales AM, Jaworski JN, Segalman RA, Zuckermann RN. Hierarchical self-assembly of a biomimetic diblock copolypeptoid into homochiral superhelices. *J Am Chem Soc.* 2010; 132: 16112–16119. [PubMed: 20964429]
108. Hule RA, Nagarkar RP, Hammouda B, Schneider JP, Pochan DJ. Dependence of self-assembled peptide hydrogel network structure on local fibril nanostructure. *Macromolecules.* 2009; 42: 7137–7145. DOI: 10.1021/ma9003242 [PubMed: 21566682]
109. Lamm MS, Rajagopal K, Schneider JP, Pochan DJ. Laminated morphology of nontwisting  $\beta$ -sheet fibrils constructed via peptide self-assembly. *J Am Chem Soc.* 2005; 127: 16692–16700. [PubMed: 16305260]
110. Barritt JD, Younan ND, Viles JH. N-terminally truncated amyloid- $\beta$ (11–40/42) cofibrillizes with its full-length counterpart: implications for Alzheimer's disease. *Angew Chem Int Ed.* 2017; 56: 9816–9819. [PubMed: 28609583]
111. Ni R, Chau Y. Tuning the inter-nanofibril interaction to regulate the morphology and function of peptide/ DNA co-assembled viral mimics. *Angew Chem int Ed.* 2017; 56: 9356–9360. [PubMed: 28643379]
112. Raymond DM, Nilsson BL. Multicomponent peptide assemblies. *Chem Soc Rev.* 2018; 47: 3659–3720. DOI: 10.1039/c8cs00115d [PubMed: 29697126]
113. Liu K, et al. Peptide-induced hierarchical long-range order and photocatalytic activity of porphyrin assemblies. *Angew Chem int Ed.* 2015; 54: 500–505. [PubMed: 25377526]
114. Zhou M, et al. Self-assembled peptide-based hydrogels as scaffolds for anchorage-dependent cells. *Biomaterials.* 2009; 30: 2523–2530. [PubMed: 19201459]
115. Ji W, et al. Regulating higher-order organization through the synergy of two self-sorted assemblies. *Angew Chem Int Ed.* 2018; 57: 3636–3640. [PubMed: 29411922]
116. Inostroza-Brito KE, et al. Co-assembly, spatiotemporal control and morphogenesis of a hybrid protein-peptide system. *Nat Chem.* 2015; 7: 897. [PubMed: 26492010]
117. Ni R, Chau Y. Structural mimics of viruses through peptide/DNA co-assembly. *J Am Chem Soc.* 2014; 136: 17902–17905. [PubMed: 25389763]
118. Jiang T, et al. Structurally ordered nanowire formation from co-assembly of DNA origami and collagen-mimetic peptides. *J Am Chem Soc.* 2017; 139: 14025–14028. [PubMed: 28949522]
119. Xing P, Li P, Chen H, Hao A, Zhao Y. Understanding pathway complexity of organic micro/nanofiber growth in hydrogen-bonded coassembly of aromatic amino acids. *ACS Nano.* 2017; 11: 4206–4216. [PubMed: 28368572]

120. Wang F, Feng C-L. Stoichiometry-controlled inversion of supramolecular chirality in nanostructures co-assembled with bipyridines. *Chem Eur J.* 2017; 24: 1509–1513. [PubMed: 29271005]
121. Wang F, Feng C-L. Metal-ion-mediated supramolecular chirality of l-phenylalanine based hydrogels. *Angew Chem Int Ed.* 2018; 57: 5655–5659. [PubMed: 29571216]
122. Liu G-F, Liu J, Feng C-L, Zhao Y. Unexpected right-handed helical nanostructures co-assembled from l-phenylalanine derivatives and achiral bipyridines. *Chem Sci.* 2017; 8: 1769–1775. DOI: 10.1039/c6sc04808k [PubMed: 29780452]
123. Liu G-F, Zhu L-Y, Ji W, Feng C-L, Wei Z-X. Inversion of the supramolecular chirality of nanofibrous structures through co-assembly with achiral molecules. *Angew Chem Int Ed.* 2015; 55: 2411–2415. [PubMed: 26663528]
124. Wang J-X, et al. Controlled arrays of self-assembled peptide nanostructures in solution and at interface. *Langmuir.* 2013; 29: 6996–7004. [PubMed: 23663135]
125. Freeman R, et al. Reversible self-assembly of superstructured networks. *Science.* 2018; 362: 808–813. DOI: 10.1126/science.aat6141 [PubMed: 30287619]
126. Tao F, Han Q, Liu K, Yang P. Tuning crystallization pathways through the mesoscale assembly of biomacromolecular nanocrystals. *Angew Chem Int Ed.* 2017; 56: 13440–13444. [PubMed: 28841270]
127. Lara C, Adamcik J, Jordens S, Mezzenga R. General self-assembly mechanism converting hydrolyzed globular proteins into giant multistranded amyloid ribbons. *Biomacromolecules.* 2011; 12: 1868–1875. [PubMed: 21466236]
128. Lashuel HA, LaBrenz SR, Woo L, Serpell LC, Kelly JW. Protofilaments, filaments, ribbons, and fibrils from peptidomimetic self-assembly: implications for amyloid fibril formation and materials science. *J Am Chem Soc.* 2000; 122: 5262–5277. [PubMed: 22339465]
129. Yang S, et al. Giant capsids from lattice self-assembly of cyclodextrin complexes. *Nat Commun.* 2017; 8: 15856. doi: 10.1038/ncomms15856 [PubMed: 28631756]
130. Van Driessche AES, et al. Molecular nucleation mechanisms and control strategies for crystal polymorph selection. *Nature.* 2018; 556: 89–94. [PubMed: 29620730]
131. Würthner F, et al. Perylene bisimide dye assemblies as archetype functional supramolecular materials. *Chem Rev.* 2016; 116: 962–1052. [PubMed: 26270260]
132. Chen S, Slattum P, Wang C, Zang L. Selfassembly of perylene imide molecules into 1D nanostructures: methods, morphologies, and applications. *Chem Rev.* 2015; 115: 11967–11998. [PubMed: 26441294]
133. Zhang X, Görl D, Stepanenko V, Würthner F. Hierarchical growth of fluorescent dye aggregates in water by fusion of segmented nanostructures. *Angew Chem Int Ed.* 2014; 53: 1270–1274. [PubMed: 24352910]
134. Görl D, Zhang X, Stepanenko V, Würthner F. Supramolecular block copolymers by kinetically controlled co-self-assembly of planar and core-twisted perylene bisimides. *Nat Commun.* 2015; 6: 7009. doi: 10.1038/ncomms8009 [PubMed: 25959777]
135. Percec V, et al. Self-repairing complex helical columns generated via kinetically controlled self-assembly of dendronized perylene bisimides. *J Am Chem Soc.* 2011; 133: 18479–18494. [PubMed: 21967251]
136. Percec V, et al. Transformation from kinetically into thermodynamically controlled self-organization of complex helical columns with 3D periodicity assembled from dendronized perylene bisimides. *J Am Chem Soc.* 2013; 135: 4129–4148. [PubMed: 23406582]
137. Partridge BE, et al. Increasing 3D supramolecular order by decreasing molecular order. a comparative study of helical assemblies of dendronized nonchlorinated and tetrachlorinated perylene bisimides. *J Am Chem Soc.* 2015; 137: 5210–5224. [PubMed: 25830346]
138. Sahoo D, et al. Hierarchical self-organization of perylene bisimides into supramolecular spheres and periodic arrays thereof. *J Am Chem Soc.* 2016; 138: 14798–14807. [PubMed: 27758100]
139. Herbst S, et al. Self-assembly of multi-stranded perylene dye J-aggregates in columnar liquidcrystalline phases. *Nat Commun.* 2018; 9: 2646. doi: 10.1038/s41467-018-05018-6 [PubMed: 29980743]

140. Yagai S, et al. Structural and electronic properties of extremely long perylene bisimide nanofibers formed through a stoichiometrically mismatched, hydrogen-bonded complexation. *Small*. 2010; 6: 2731–2740. [PubMed: 21069756]
141. Marty R, et al. Hierarchically structured microfibers of “single stack” perylene bisimide and quaterthiophene nanowires. *ACS Nano*. 2013; 7: 8498–8508. [PubMed: 23952000]
142. Palmer LC, et al. Long-range ordering of highly charged self-assembled nanofilaments. *J Am Chem Soc*. 2014; 136: 14377–14380. [PubMed: 25255327]
143. Taden A, Landfester K, Antonietti M. Crystallization of dyes by directed aggregation of colloidal intermediates: a model case. *Langmuir*. 2004; 20: 957–961. [PubMed: 15773129]
144. Zhang C, et al. Porphyrin supramolecular 1D structures via surfactant-assisted self-assembly. *Adv Mater*. 2015; 27: 5379–5387. [PubMed: 26178274]
145. Hu J-S, Guo, Liang H-P, Wan L-J, Jiang L. Three-dimensional self-organization of supramolecular self-assembled porphyrin hollow hexagonal nanoprisms. *J Am Chem Soc*. 2005; 127: 17090–17095. [PubMed: 16316256]
146. Guo P, Chen P, Liu M. Porphyrin assemblies via a surfactant-assisted method: from nanospheres to nanofibers with tunable length. *Langmuir*. 2012; 28: 15482–15490. [PubMed: 23072662]
147. Qiu Y, Chen P, Liu M. Evolution of various porphyrin nanostructures via an oil/aqueous medium: controlled self-assembly, further organization, and supramolecular chirality. *J Am Chem Soc*. 2010; 132: 9644–9652. [PubMed: 20578772]
148. Kim T, Ham S, Lee SH, Hong Y, Kim D. Enhancement of exciton transport in porphyrin aggregate nanostructures by controlling the hierarchical self-assembly. *Nanoscale*. 2018; 10: 16438–16446. [PubMed: 30141821]
149. Xu G, Li Q, Chen X. Nanobelts of hexagonal columnar crystal lattice through ionic self-assembly. *Colloid Polym Sci*. 2015; 293: 2877–2882.
150. Li H, Guan M, Zhu G, Yin G, Xu Z. Experimental observation of fullerene crystalline growth from mesocrystal to single crystal. *Cryst Growth Des*. 2016; 16: 1306–1310.
151. Zhang X, Takeuchi M. Controlled fabrication of fullerene C60 into microspheres of nanoplates through porphyrin-polymer-assisted self-assembly. *Angew Chem Int Ed*. 2009; 48: 9646–9651. [PubMed: 19876993]
152. Zhang X, et al. Supramolecular [60]fullerene liquid crystals formed by self-organized two-dimensional crystals. *Angew Chem Int Ed*. 2014; 54: 114–117. [PubMed: 25327867]
153. Ramos Sasselli I, Halling PJ, Ulijn RV, Tuttle T. Supramolecular fibers in gels can be at thermodynamic equilibrium: a simple packing model reveals preferential fibril formation versus crystallization. *ACS Nano*. 2016; 10: 2661–2668. [PubMed: 26812130]
154. Palermo V, Samorì P. Molecular self-assembly across multiple length scales. *Angew Chem Int Ed*. 2007; 46: 4428–4432. [PubMed: 17497615]
155. Knowles TP, et al. Role of intermolecular forces in defining material properties of protein nanofibrils. *Science*. 2007; 318: 1900–1903. [PubMed: 18096801]
156. Mendes AC, Baran ET, Reis RL, Azevedo HS. Self-assembly in nature: using the principles of nature to create complex nanobiomaterials. *Wiley Interdiscip Rev Nanomed Nanobiotechnol*. 2013; 5: 582–612. [PubMed: 23929805]
157. Ulijn RV, Smith AM. Designing peptide based nanomaterials. *Chem Soc Rev*. 2008; 37: 664–675. [PubMed: 18362975]
158. Fichman G, et al. Spontaneous structural transition and crystal formation in minimal supramolecular polymer model. *Sci Adv*. 2016; 2: e1500827. doi: 10.1126/sciadv.1500827 [PubMed: 26933679]
159. Dudukovic NA, Hudson BC, Paravastu AK, Zukoski CF. Self-assembly pathways and polymorphism in peptide-based nanostructures. *Nanoscale*. 2018; 10: 1508–1516. [PubMed: 29303206]
160. Banwell EF, et al. Rational design and application of responsive  $\alpha$ -helical peptide hydrogels. *Nat Mater*. 2009; 8: 596–600. DOI: 10.1038/nmat2479 [PubMed: 19543314]
161. González-Rodríguez D, et al. G-quadruplex selfassembly regulated by coulombic interactions. *Nat Chem*. 2009; 1: 151–155. [PubMed: 21378828]

162. Faul CFJ, Antonietti M. Ionic self-assembly: facile synthesis of supramolecular materials. *Adv Mater.* 2003; 15: 673–683.
163. Rehm TH, Schmuck C. Ion-pair induced selfassembly in aqueous solvents. *Chem Soc Rev.* 2010; 39: 3597–3611. [PubMed: 20552123]
164. Jeffrey, GA, Saenger, W. *Hydrogen Bonding in Biological Structures.* Springer Science & Business Media; 2012.
165. Brunsveld L, Folmer BJB, Meijer EW, Sijbesma RP. Supramolecular polymers. *Chem Rev.* 2001; 101: 4071–4098. [PubMed: 11740927]
166. Krieg E, Bastings MMC, Besenius P, Rybtchinski B. Supramolecular polymers in aqueous media. *Chem Rev.* 2016; 116: 2414–2477. [PubMed: 26727633]
167. Grimme S. Do special noncovalent  $\pi$ - $\pi$  stacking interactions really exist? *Angew Chem Int Ed.* 2008; 47: 3430–3434. [PubMed: 18350534]
168. Martinez CR, Iverson BL. Rethinking the term “pi-stacking”. *Chem Sci.* 2012; 3: 2191–2201.
169. Cockroft SL, Hunter CA, Lawson KR, Perkins J, Urch CJ. Electrostatic control of aromatic stacking interactions. *J Am Chem Soc.* 2005; 127: 8594–8595. [PubMed: 15954755]
170. Chandler D. Interfaces and the driving force of hydrophobic assembly. *Nature.* 2005; 437: 640–647. [PubMed: 16193038]
171. Ball P. Water as an active constituent in cell biology. *Chem Rev.* 2008; 108: 74–108. [PubMed: 18095715]
172. Tao J, et al. Energetic basis for the molecular-scale organization of bone. *Proc Natl Acad Sci USA.* 2015; 112: 326. doi: 10.1073/pnas.1404481112 [PubMed: 25540415]
173. Manoharan VN. Colloidal matter: packing, geometry, and entropy. *Science.* 2015; 349: 1253751. [PubMed: 26315444]
174. Onsager L. The effects of shape on the interaction of colloidal particles. *Ann N Y Acad Sci.* 1949; 51: 627–659.
175. Needleman DJ, et al. Higher-order assembly of microtubules by counterions: from hexagonal bundles to living necklaces. *Proc Natl Acad Sci USA.* 2004; 101: 16099–16103. DOI: 10.1073/pnas.0406076101 [PubMed: 15534220]
176. Yao Z, Olvera de la Cruz M. Electrostatic repulsion-driven crystallization model arising from filament networks. *Phys Rev E.* 2013; 87: 042605. [PubMed: 23679441]
177. Voorhees PW. The theory of Ostwald ripening. *J Stat Phys.* 1985; 38: 231–252.
178. De Yoreo JJ, et al. Crystallization by particle attachment in synthetic, biogenic, and geologic environments. *Science.* 2015; 349: aaa6760. [PubMed: 26228157]
179. Bishop KJM, Wilmer CE, Soh S, Grzybowski BA. Nanoscale forces and their uses in self-assembly. *Small.* 2009; 5: 1600–1630. [PubMed: 19517482]

**Paracrystals**

A kind of solid-phase state exhibiting short-range and medium-range ordering in the lattice (similar to liquid crystal phases) but lacking long-range ordering in at least one direction.



**Ferrofluid**

A kind of liquid that becomes strongly magnetized in the presence of a magnetic field.

**Solvothermal treatment**

An approach for preparing crystalline materials with micro/nanostructures such as metals, polymers and semiconductors from a nonaqueous solution in an autoclave (a thick-walled steel vessel) at high temperature and pressure.

### **Optical waveguiding**

A physical property possessed by a perfect and smooth physical structure that can guide electromagnetic waves in the optical spectrum.

**Nematic liquid crystal**

A kind of thermotropic liquid crystal in which the molecules are in a definite order or pattern.

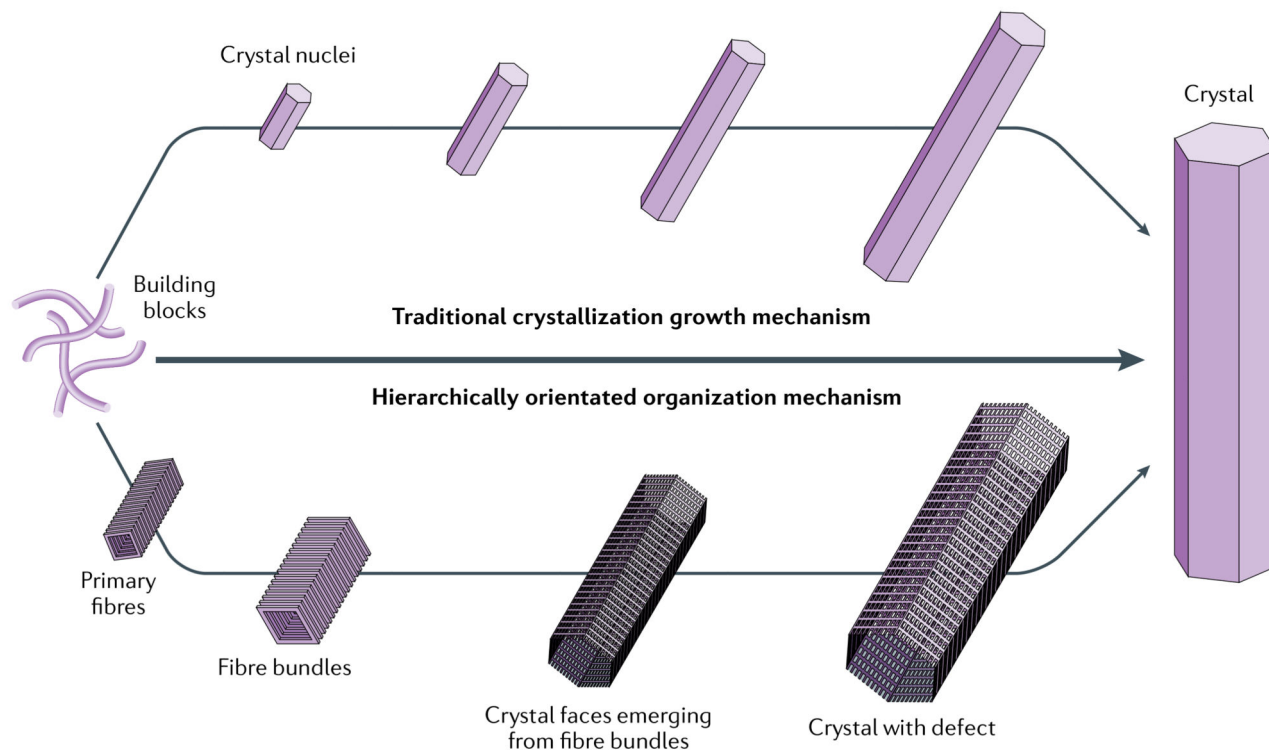


**Fig. 1. Classical and hierarchically oriented organization self-assembly mechanism.**

Schematic comparison between the traditional crystallization growth mechanism and the proposed hierarchically oriented organization mechanism.

The former mechanism is based on the diffusion-controlled Ostwald ripening by which components of the discontinuous phase diffuse from smaller to larger through the continuous phase, whereas the latter is a growth process based on the entropic ordering of the primary nanostructures, such as primary fibres and other nanostructures.

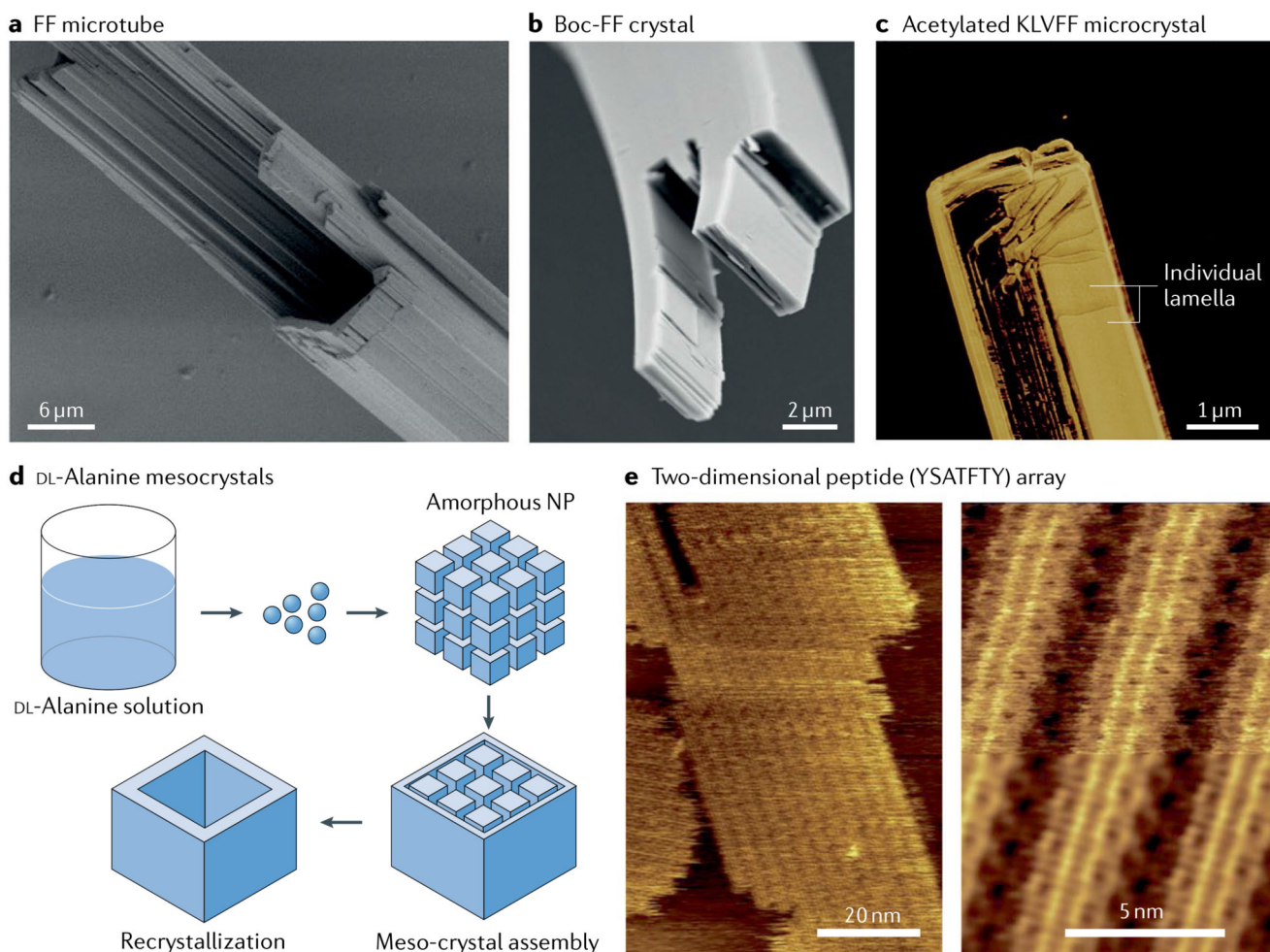


**Fig. 2. Hierarchically oriented crystallization of linear short peptides.**

**a** | Scanning electron microscopy images of hexagonal peptide microtubes formed by the high-order assembly of diphenylalanine (FF) nanotubes<sup>13</sup>. **b** | Laminated crystal structures resulting from *tert*-butoxycarbonyl diphenylalanine (Boc-FF) high-order self-assembly that results in mechanical flexibility<sup>7</sup>. **c** | Atomic force microscopy (AFM) image of acetylated KLVFF microcrystals exhibiting a lamellar structure<sup>27</sup>. **d** | Schematic illustration of the oriented organization of nanocrystals that leads to the formation of hollow DL-alanine mesocrystals<sup>34</sup>. **e** | In situ AFM images of MoSBP1 assemblies constrained on the MoS<sub>2</sub> (0001) surface (left) showing parallel rows with a periodicity of 4.1 nm (right)<sup>41</sup>. NP, nanoparticle. Part **a** is adapted with permission from REF.<sup>13</sup>, Wiley-VCH. Part **b** is adapted with permission from REF.<sup>7</sup>, Wiley-VCH. Part **c** is adapted with permission from REF.<sup>27</sup>, ACS. Part **d** is adapted with permission from REF.<sup>34</sup>, ACS. Part **e** is adapted with permission from REF.<sup>41</sup>, AAAS.



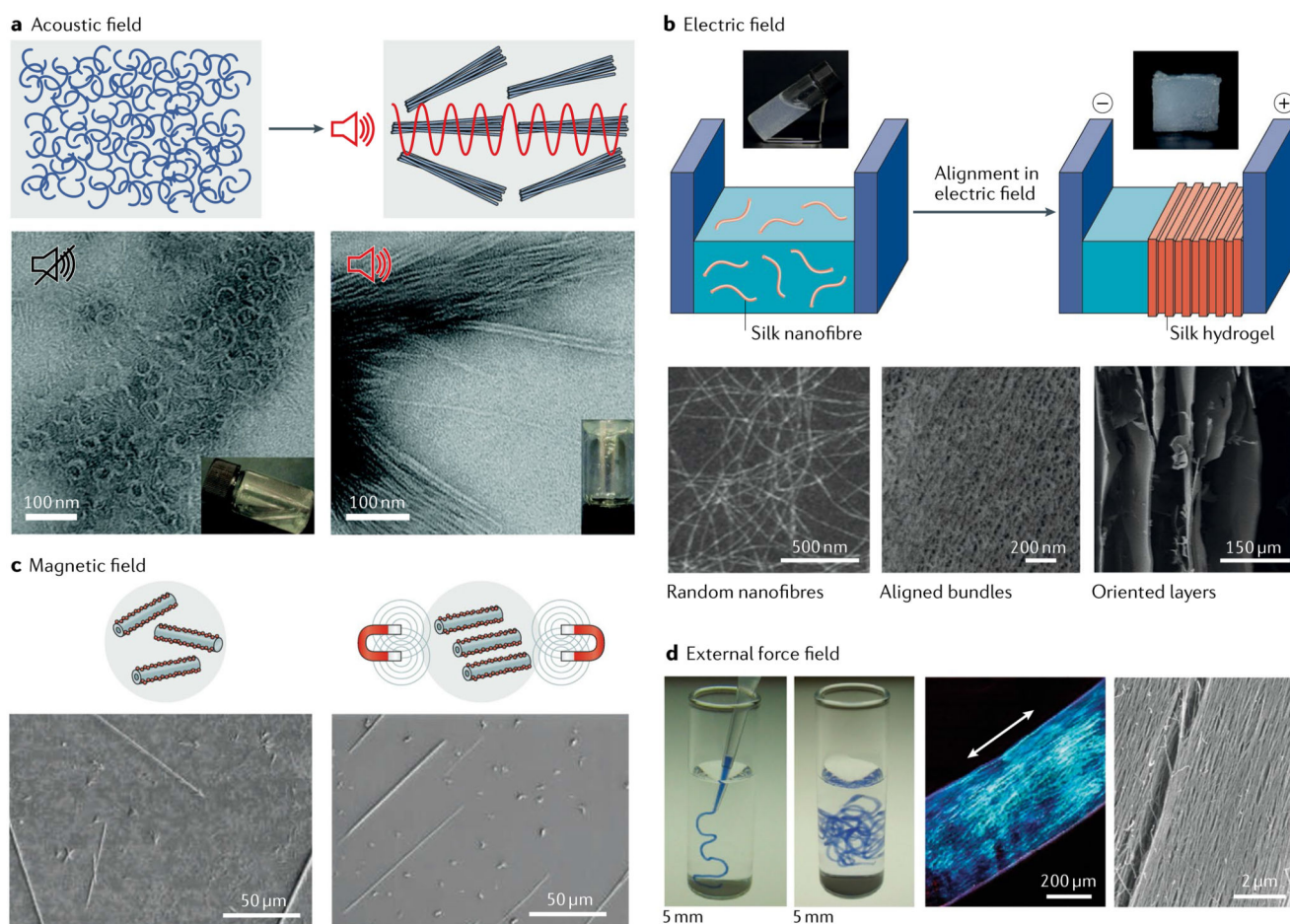


**Fig. 3. External stimuli-induced oriented alignment of short peptide self-assembly.**

**a** | Schematic (top) and scanning electron microscopy (SEM) images (bottom) of self-assembly and alignment of tripeptide (DFFD and <sup>D</sup>FFI) microfibrillar structures by in situ ultrasonication<sup>48</sup>. **b** | Schematic (top) and transmission electron microscopy images (bottom) of the electric field-induced hierarchical alignment of silk nanofibres and the resulting anisotropic hydrogel<sup>49</sup>. **c** | Schematic (top) and SEM images (bottom) of magnetic field-induced alignment of the self-assembled diphenylalanine dipeptide nanotubes<sup>15</sup>. **d** | Noodle-like strings (left) obtained by injecting aqueous peptide amphiphilic (C<sub>15</sub>H<sub>31</sub>CO-VVVAEEEE(COOH)) solution into phosphate-buffered saline. Uniform birefringence and aligned nanofibre bundles (right) induced by the shear force<sup>51</sup>. Part **a** is reproduced with permission from REF<sup>48</sup>, RSC. Part **b** is adapted with permission from REF<sup>49</sup>, Wiley-VCH. Part **c** is adapted from REF.<sup>15</sup>, Springer Nature Limited. Part **d** is adapted from REF.<sup>51</sup>, Springer Nature Limited.

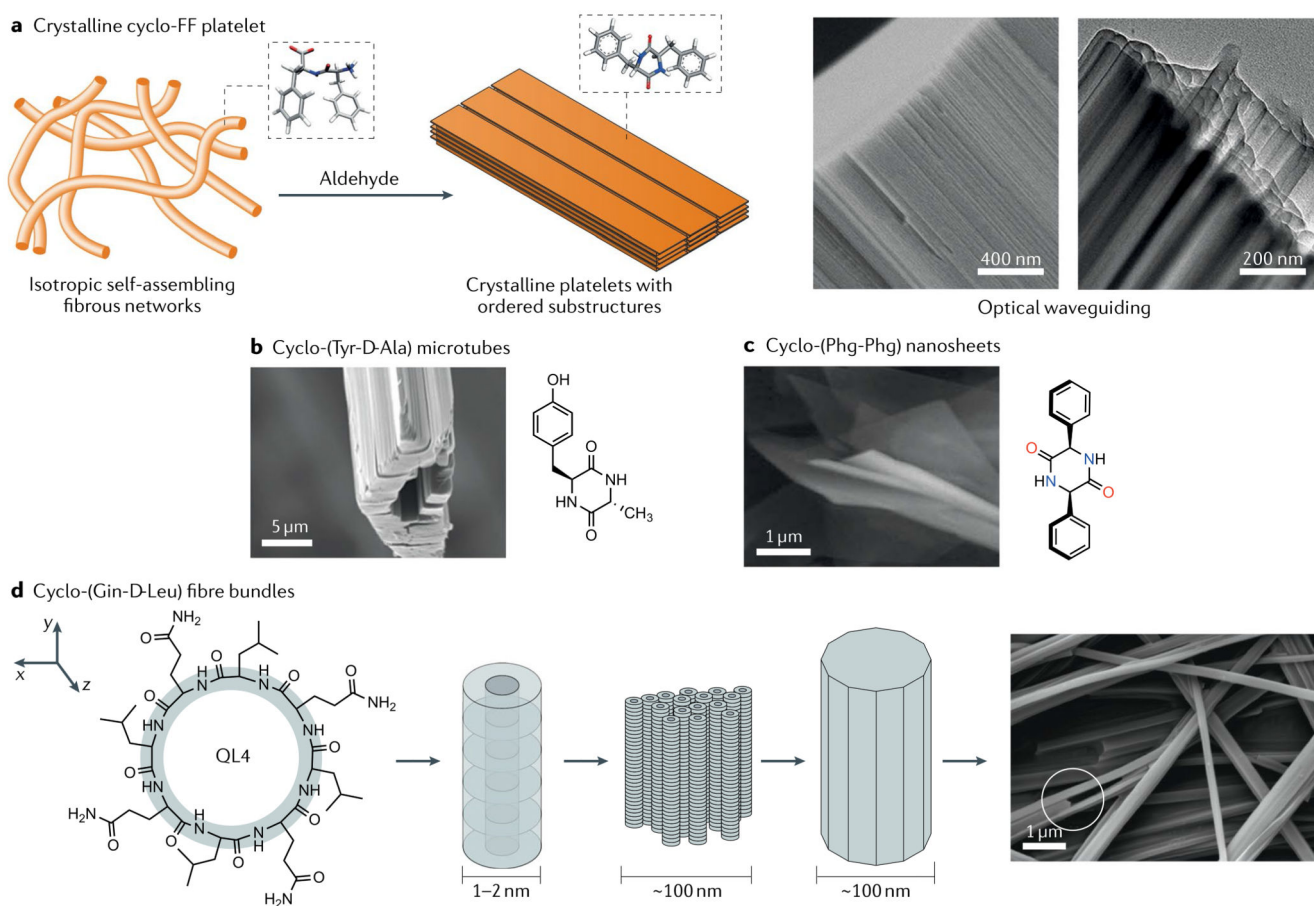


**Fig. 4. Hierarchically oriented crystallization of cyclic peptides.**

**a** | Long-range oriented crystallization of cyclo-diphenylalanine (cyclo-FF) can be achieved by the introduction of aldehyde or solvothermal treatment of a linear FF gel (schematic on the left). Aldehyde facilitates the intramolecular cyclization of linear FF and the subsequent phase transition from gels to crystals. Scanning electron microscopy and transmission electron microscopy (TEM) images clearly demonstrate the hierarchically oriented organization patterns (panels on the right)<sup>63</sup>. **b** | Crystalline microtubes composed of layered structures of cyclo-(L-Tyr-D-Ala)<sup>71</sup>. **c** | Mesosheets composed of layered structures of cyclo-(L-Phg-L-Phg)<sup>72</sup>. **d** | Schematics of the formation of bundled fibres of cyclo-([G-D-L]<sub>4</sub>) (QL4) (left). The hierarchical order is further confirmed by the high-resolution TEM image<sup>78</sup>. Part **a** is adapted with permission from REF.<sup>63</sup>, Wiley-VCH. Part **b** is adapted with permission from REF.<sup>71</sup>, ACS. Part **c** is adapted with permission from spontaneous self-assembly of designed cyclic dipeptide (Phg-Phg) into two-dimensional nano- and mesosheets, Govindaraju, T. et al. *Supramolecular Chemistry* (2011) REF.<sup>72</sup>, reprinted by permission of the publisher (Taylor & Francis Ltd, <http://www.tandfonline.com>). Part **d** is adapted with permission from REF.<sup>78</sup>, ACS.

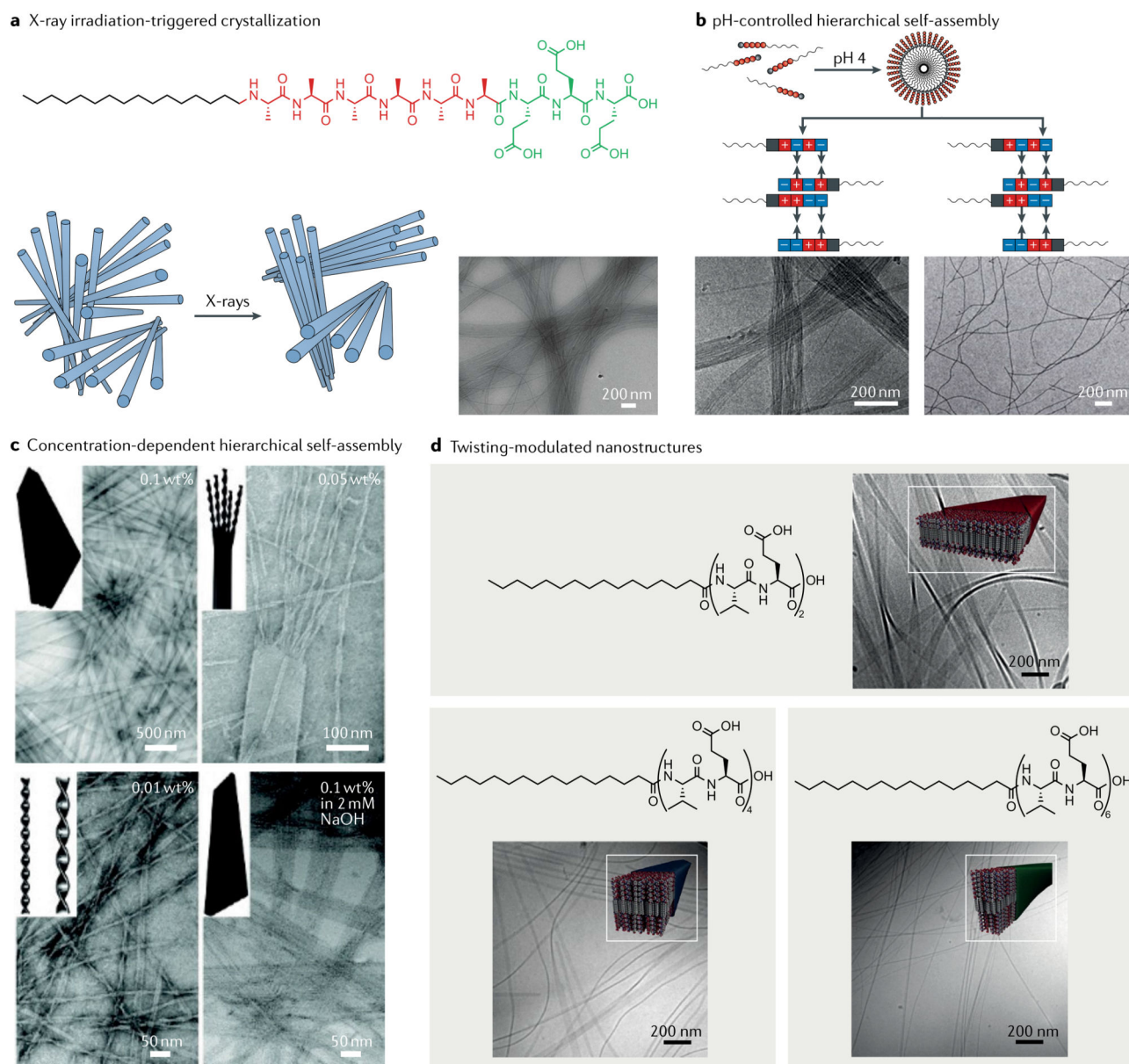


**Fig. 5. Hierarchical self-assembly and crystallization of amphiphilic peptides.**

**a** | X-ray-triggered phase transition of amphiphilic peptide filaments from a disordered phase to a hexagonally ordered phase as shown in the schematic (left). The formation of filament bundles is confirmed by cryo-transmission electron microscopy (right)<sup>11</sup>. **b** | pH-controlled hierarchical self-assembly of amphiphilic peptide (top left) ranging from micelles (top right) to nanofiber bundles (middle-left and bottom-left) to nanofibers (middle-right and bottom-right). The nanofiber bundles are the result of the complementary-attractive interactions between the surface regions of interdigitating peptide amphiphiles, and well-dispersed nanofibers are the result of the complementary repulsive interactions<sup>84</sup>. **c** | Concentration-dependent and pH-dependent morphology transformation of a flat amphiphilic peptide



nanobelt into twisted nanoribbons. Transmission electron microscopy images clearly display this structural evolution from a flat nanobelt to a split nanobelt with a broom morphology. Decreasing the monomer concentration leads to the formation of twisted nanoribbons as well as the transformation from a flat nanobelt to a grooved nanobelt with parallel nanochannels. These images reveal that the flat nanobelts formed in a hierarchically oriented organization manner<sup>85</sup>. **d** | Hierarchical self-assembly of amphiphilic peptides containing variable numbers of valine-glutamic acid dimeric repeats<sup>92</sup>. Part **a** is adapted with permission from REF.<sup>11</sup>, AAAS. Part **b** is adapted with permission from REF.<sup>84</sup>, ACS. Part **c** is adapted with permission from REF.<sup>85</sup>, ACS. Part **d** is adapted with permission from REF.<sup>92</sup>, ACS.

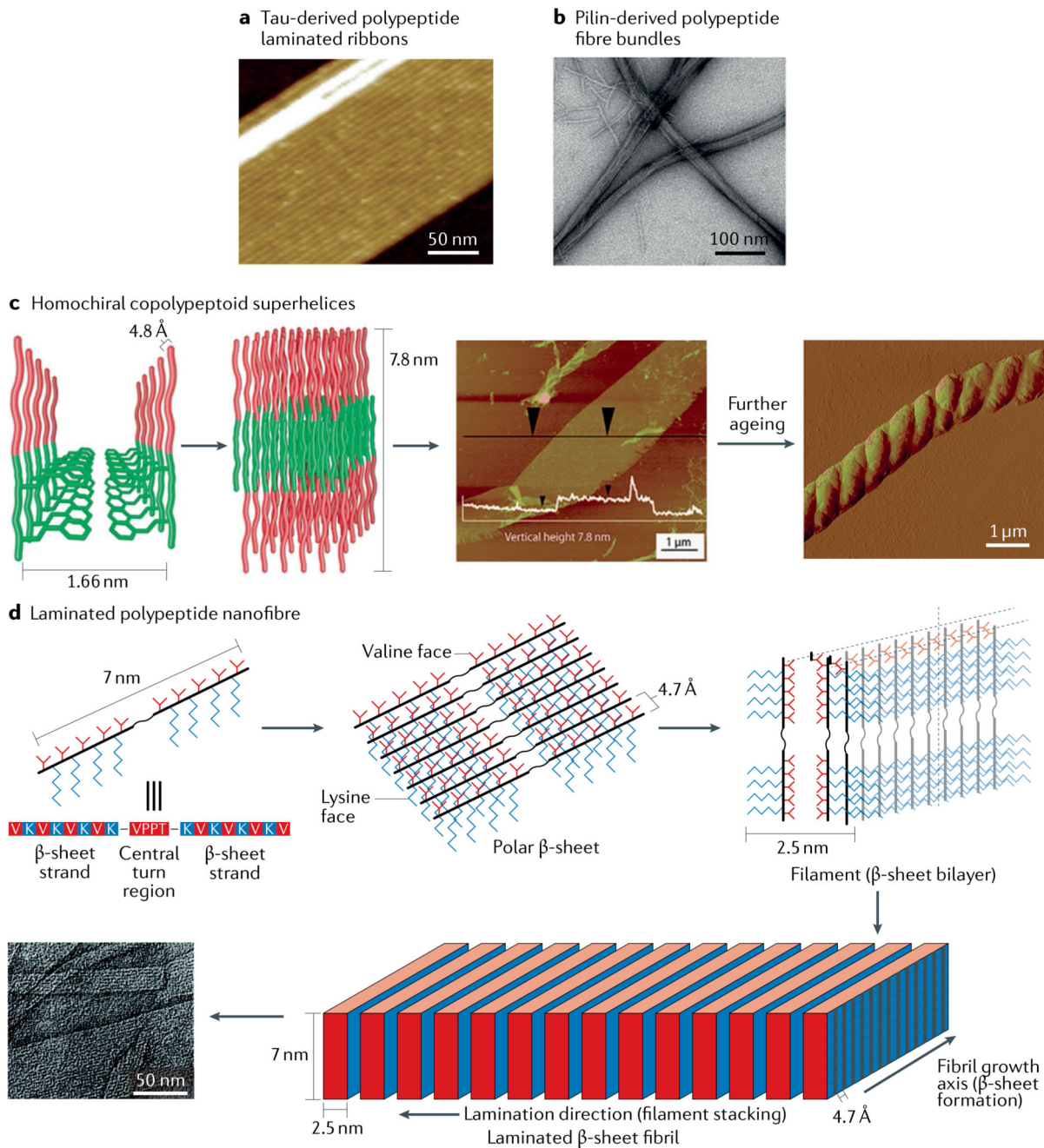


**Fig. 6. Hierarchically oriented polypeptide self-assembly.**

**a** | Multistranded ribbons self-assembled from a tau-derived polypeptide<sup>103</sup>. **b** | Fibre bundles self-assembled from a pilin-based polypeptide<sup>105</sup>. **c** | Helix formed from the lamellar stacked nanosheets of a diblock copolypeptoid. In the proposed hierarchical self-assembly model (left), the hydrophobic and hydrophilic portions of the chain are represented by green and red, respectively. Atomic force microscopy (AFM) image of the obtained layered structure (centre); the white overlay indicates the vertical height of the structure. AFM image of the helical structure that forms after further ageing (right)<sup>107</sup>. **d** | Flat

fibril laminates formed through lateral association of  $\beta$ -sheet filaments. Polar  $\beta$ -sheets (top middle) with different hydrophobic (valine) and hydrophilic (lysine) faces are first formed from the self-assembly of polypeptide (top left) exhibiting an extended  $\beta$ -strand conformation. Subsequently, filaments (top right) are formed through the hydrophobic collapse of  $\beta$ -sheets. Lateral stacking of these filaments results in the formation of flat fibrils (bottom)<sup>109</sup>. Part **a** is reproduced with permission from REF.<sup>103</sup>, Wiley-VCH. Part **b** is adapted from REF.<sup>105</sup>, Springer Nature Limited. Part **c** is adapted with permission from REF.<sup>107</sup>, ACS. Part **d** is adapted with permission from REF<sup>109</sup>, ACS.



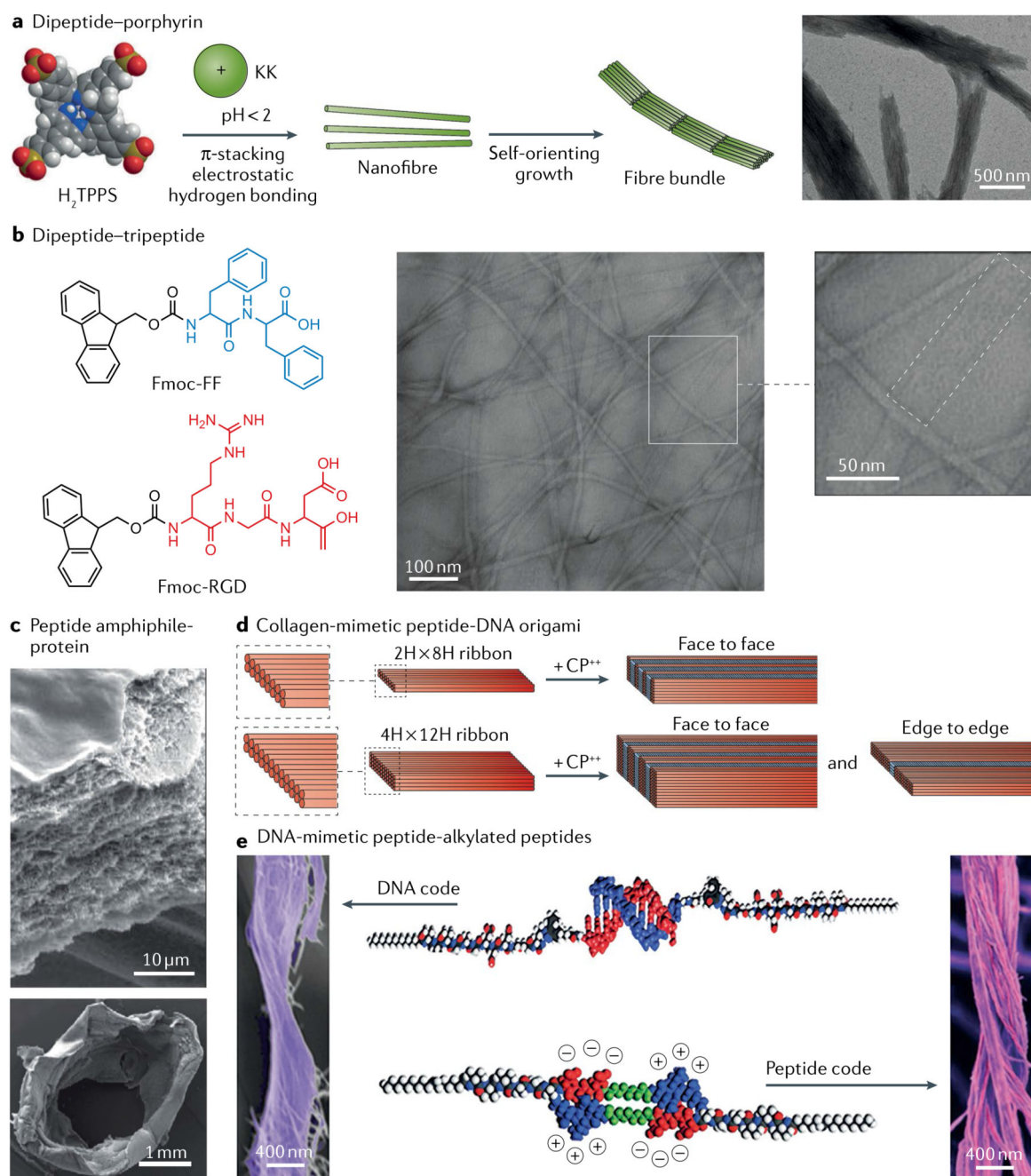


**Fig. 7. Hierarchically oriented organization in peptide-containing co-assembly systems.**  
**a** | Long-range ordered nanofibre bundles assembled from a dipeptide (KK)–porphyrin co-assembly system due to the balance between electrostatic repulsion and van der Waals attraction<sup>113</sup>. **b** | Flat ribbons of 9-fluorenylmethyloxycarbonyl (Fmoc)–diphenylalanine (FF) and Fmoc–RGD co-assemblies comprising laterally aligned fine fibrils about 3 nm in diameter, as observed by fast Fourier transform analysis<sup>114</sup>. **c** | A protein–peptide co-assembly membrane containing elastin-like polypeptides and an amphiphilic peptide demonstrates pronounced nanofibrous multilayered architecture, as shown by scanning

electron microscopy images of a cross-section of the membrane (top). The membrane can further evolve into tubular structures with simultaneously spatiotemporal control (bottom)<sup>116</sup>. **d** | Co-assembly of collagen-mimetic peptides (CP<sup>++</sup>) and DNA origami yields the formation of nanowires with repeating periodicity of about 10 nm through face-to-face or edge-to-edge packing modes<sup>118</sup>. **e** | Bundles of intertwined fibres formed through co-assembly of DNA-mimetic peptide amphiphiles (top) and alkylated peptides (bottom)<sup>125</sup>. Part **a** is adapted with permission from REF.<sup>113</sup>, Wiley-VCH. Part **b** is adapted with permission from REF.<sup>114</sup>, Elsevier. Part **c** is reproduced from REF.<sup>116</sup>, Springer Nature Limited. Part **d** is reproduced with permission from REF.<sup>118</sup>, ACS. Part **e** is reproduced with permission from REF.<sup>125</sup>, AAAS.

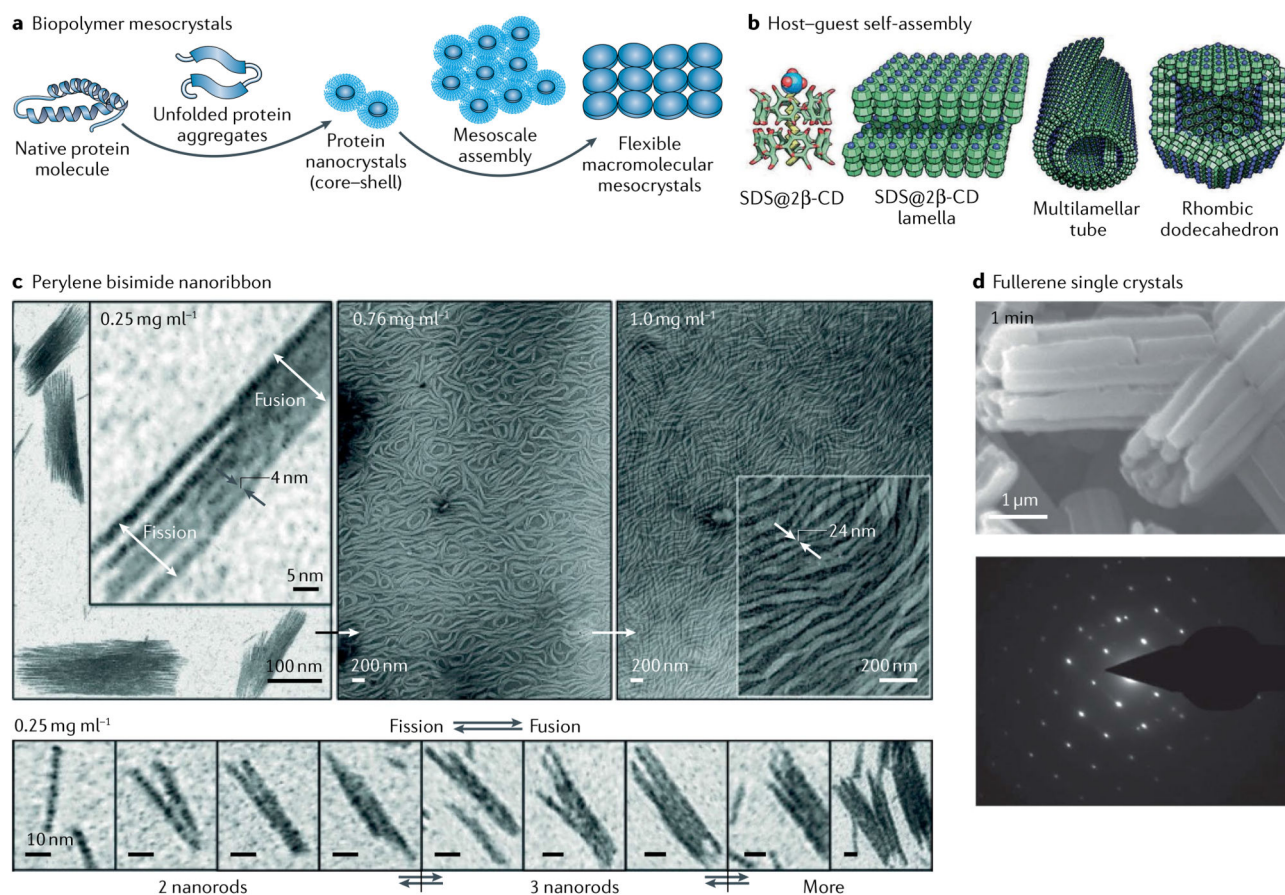


**Fig. 8. Hierarchically oriented organization in extended self-assembly systems.**

**a** | Formation and self-assembly of protein nanocrystals to form biopolymer mesocrystals<sup>126</sup>. **b** | Concentration-dependent hierarchical host-guest selfassembly based on cyclodextrin–SDS complexes from lamellar (50–25 wt%) to tubular (25–6 wt%) and to polyhedral (6–4 wt%) structures<sup>129</sup>. **c** | Nanoribbons self-assembled from hierarchically oriented nanorods of amphiphilic perylene bisimide with the gradual increase of the monomer concentration. Such a hierarchically oriented fusion and fission process between nanorods is clearly demonstrated at a certain concentration (0.25 mg ml<sup>-1</sup>; bottom)<sup>133</sup>. **d** | Fullerene single crystal grown from the mesocrystal stacked by highly oriented nanocrystals. The bundles with strip-like structures reveal an intermediate structure between the nanocrystal and single crystals. The bright dots on selected area electron diffraction demonstrate the formation of perfect crystalline structure<sup>150</sup>. Part **a** is reproduced with permission from REF.<sup>126</sup>, Wiley-VCH. Part **b** is reproduced from REF.<sup>129</sup>, CC-BY-4.0. Part **c** is reproduced with permission from REF.<sup>133</sup>, Wiley-VCH. Panel **d** is reproduced with permission from REF.<sup>150</sup>, ACS.

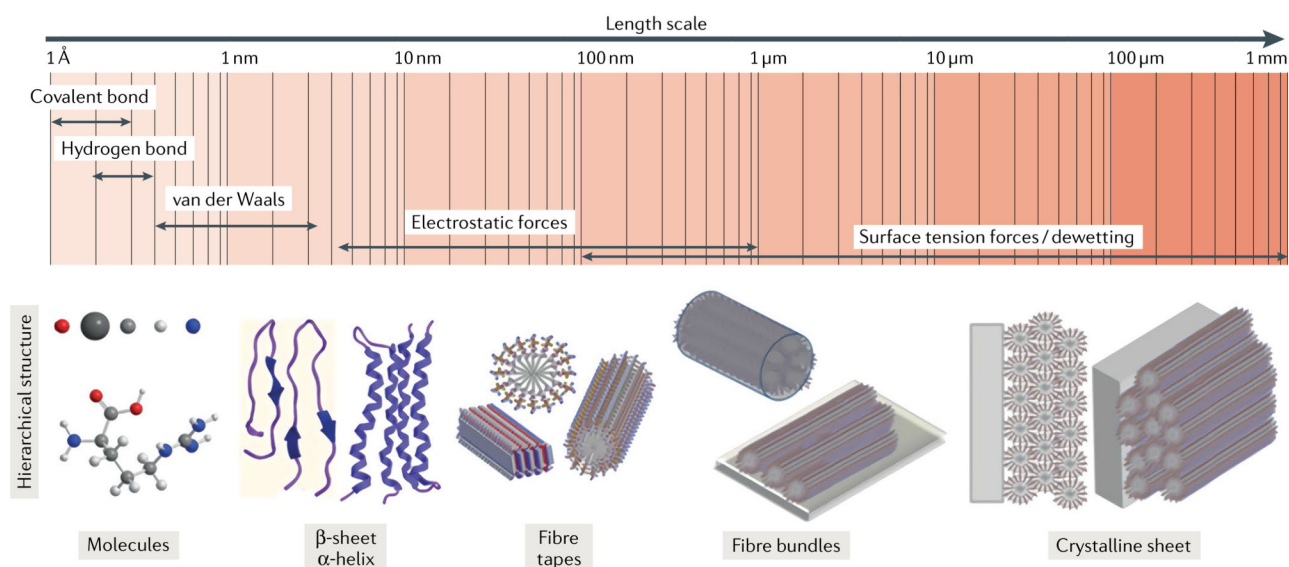


**Fig. 9. Intermolecular interactions involved in multiscale hierarchical self-assembly of peptides.** Different intermolecular interactions are involved in the multiscale hierarchical self-assembly of peptides. Different intermolecular interactions have distinct roles for the hierarchical self-assembly process stepping at different scales, from elementary molecules to secondary structures such as  $\beta$ -sheets and  $\alpha$ -helices, to fibres and fibre bundles, and even to crystalline structures. It should be noted that intermolecular  $\beta$ -sheets and helices are often formed in short peptide self-assembly, whereas intramolecular sheets and helices can be formed in polypeptide and protein self-assembly. Reproduced with permission from REF.<sup>156</sup>, Wiley-VCH.



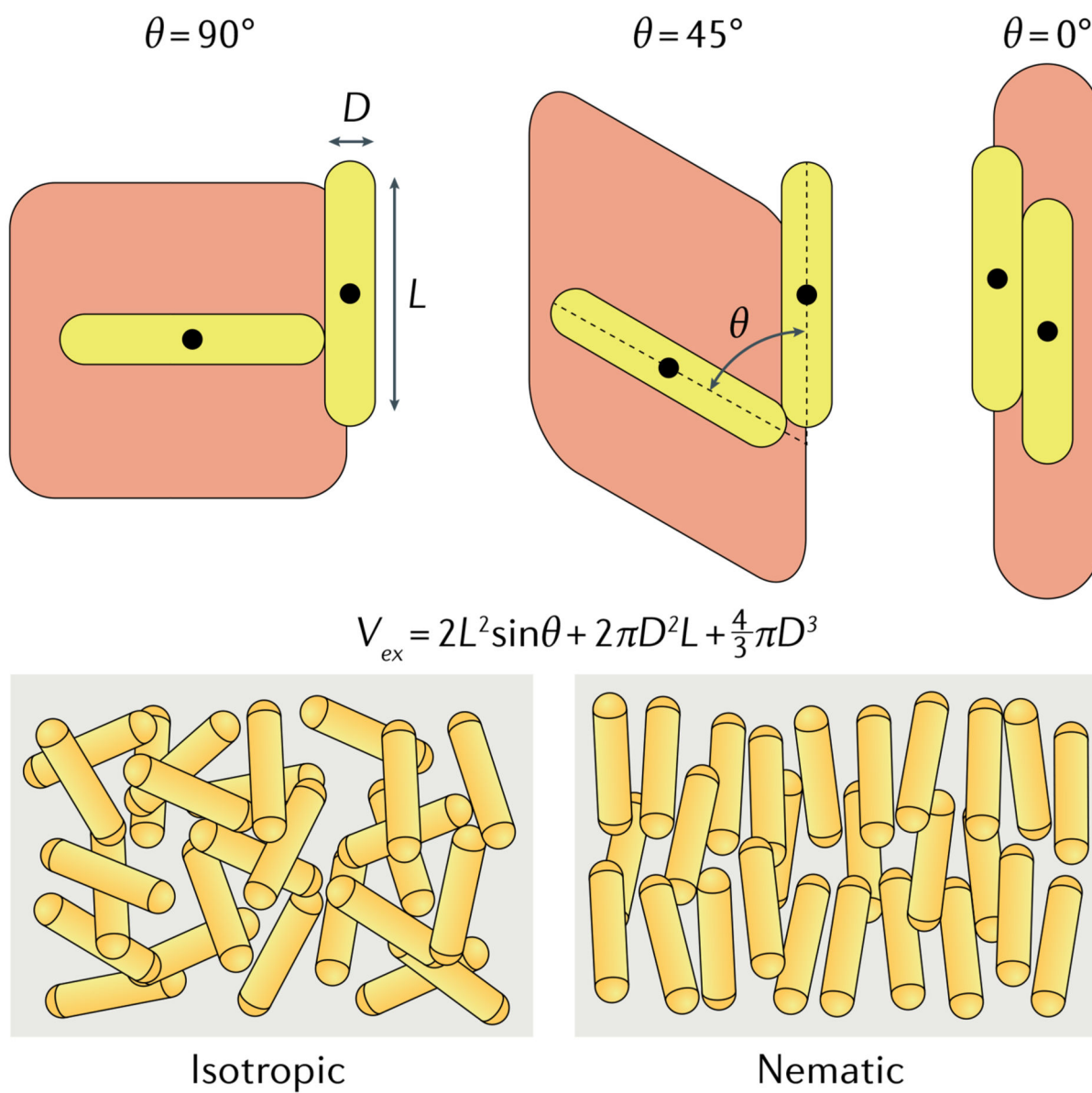


**Fig. 10. The isotropic–nematic phase transition is entropically driven.**

Parallel arrangement of hard rods in solution results in the minimum excluded volume (red-shaded area), leading to the entropy maximum of the total system. This increases the translational freedom of rods and solvents, which facilitates the phase isotropic to nematic transition. Reproduced with permission from REF.<sup>179</sup>, Wiley-VCH.